Master Thesis

Variability in hydrochemical properties and composition of the dense water in the Faroese Channels

by

Astri Horge Glindø

Geophysical Institute

Department of Chemical Oceanography

University of Bergen

May 2018

Acknowledgement

I would like to thank the University of Bergen for the opportunity to study and experience the Arctic at UNIS, which gave me the inspiration to pursue this thesis.

My heartfelt appreciation goes out to my two supervisors, Emil Jeansson and Kjetil Våge. With great enthusiasm and knowledge they have guided me through the deep waters of the Faroese Channels, quickly responding to any query at any hour. Thank you.

Lastly, I would like to thank family and friends for encouragement, support, and genuine interest in my work.

Abstract

The temporal variability in deep water properties and composition in both Faroe-Shetland and Faroe Bank Channel were examined in June 2002, July 2009, and April 2015. Differences in the water column structure and property were observed between the two locations, influenced by difference in Atlantic inflows and by mixing processes along the channels. However, the source waters MNAW, MEIW, ISAIW, and NSDW described the deep water well at both sites at the three specified times. The seasonal shift between summer 2002/2009 and spring 2015 was traced in the surface layer of the water column. From available observations, the deep water in the channels experienced an increase in salinity between 2002 and 2015. The Faroe Bank warmed especially in the lightest part of the deep water in 2015 due to increased Atlantic influence at this location. Enhanced oxygen values in 2015 together with a minimal fraction of ISAIW found in the deep water composition indicate the presence of a different source and an interchanging water supply to the channels. Source water fractions reveal no temporal variations.

Contents

Chapter 1

Background

1.1 Motivation

The North Atlantic Current is an extension of the Gulf Stream and carries warm surface water from equatorial latitudes towards polar latitudes. As the atmospheric temperature drops towards polar latitudes, the heat within the water is released. The result is a mild climate in a region otherwise influenced by the Arctic. As the flow loses heat its density increases, while local processes and mixing further alter the water properties. The previously warm surface water is transformed into denser water. Thus, the subpolar and polar regions are domains of dense water formation. After the transformation, the now deep flow returns towards equatorial latitudes. Its pathway takes it through the Nordic Seas; the collective term for the Greenland, Iceland, and Norwegian Seas [Hurdle, 1986]. Separating the Nordic Seas and the North Atlantic Ocean is the Greenland-Scotland Ridge, which primarily allows dense water exchange between the areas through two gaps; the Denmark Strait and the Faroese Channels. Upon exit, the deep flow becomes part of the bottom current in the North Atlantic Ocean [Dickson and Brown, 1994]. This deep conversion of the previous surface flow is an important part of the Atlantic meridional overturning circulation (AMOC), one of the global ocean's circulation cells [Wunsch, 2002].

Oceanic temperatures are presently increasing, correlated to a warming atmosphere. Enhanced temperatures could lead to an increased volume of fresh water in the Arctic, due to less sea ice formation and increased supply from river outlets [Aagaard and Carmack, 1989]. Reduced salinities in the surface would strengthen the stratification of the water layers, inhibiting formation of dense water. What will the effect be on the AMOC? Kuhlbrodt et al. (2017) theorize a temporarily halt or a possible switch to another stable circulation scheme, while Caesar et al. (2018) discuss a weakening in the AMOC. According to Curry and Mauritzen (2005), an eventual shutoff by weakening is estimated to take almost two centuries, unless substantial freshwater is injected. The AMOC influence the air-sea heat exchange and water column stratification by transporting warm surface water toward polar latitudes, contribute to storage of atmospheric gases such as carbon dioxide upon deep water formation, and distribution of water masses [Kuhlbrodt et al., 2007]. Thus, any variations in this circulation system will have global ramifications and monitoring of the AMOC is without a doubt of great concern.

The Nordic Seas are home to a variety of waters which are influenced by local processes, atmospheric forcing, region-wide circulation, and inflows of both Atlantic and Arctic waters. Some of these waters have the characteristics to supply the deep branch of AMOC, but which ones depends on the variation of the previous influential processes. To measure and establish variations in the effect of these processes would be demanding. Fortunately, all water contributing to the

bottom current in the North Atlantic Ocean have to cross the Greenland-Scotland Ridge. One of the two sites which enables deep water exchange is the Faroese Channels. Examining the water flowing through here, variation in properties and composition would indicate changes in water formation in the Nordic Seas and possibly reveal which processes could influence the AMOC. This thesis proceeds with a short introduction to the Nordic Seas and its characteristics, before investigating potential variation in water properties and composition in the Faroese Channels.

1.2 Bathymetry

The Nordic Seas are separated from the Arctic Ocean by the 2600m deep Fram Strait between Greenland and Spitsbergen together with the shallow entrance to the Barents Sea between Spitsbergen and northern Norway. The Nordic Seas are further bounded by Greenland to the west and Norway to the east and isolated from the North Atlantic Ocean by the Greenland-Scotland Ridge to the south. The transfer of water between the Nordic Seas and the North Atlantic Ocean is greatly limited by the Greenland-Scotland Ridge, which has a mean depth of 500m [Hansen et al., 2001]. It consists of three distinct regions which are, from west to east; the 600m deep Denmark Strait located between Greenland and Iceland, the 500m deep Iceland-Faroe Ridge, and the Faroese Channels southwest of the Faroe Islands [Wilkenskjeld and Quadfasel, 2005].

The Nordic Seas have a total volume of approximately $5.25*10^6 km^3$, or about 0.33% of the volume of the global ocean [Aagaard et al., 1985]. It has a prominent bathymetric feature: a north-south oriented mid-ocean ridge, which divides the Nordic Seas into a warm Atlantic eastern side, an Arctic domain in the middle, and a cold Polar western side. The areas are given their names according to the water that exert the greatest influence in that region. At the latitude of Jan Mayen, the Jan Mayen Fracture Zone cuts through the mid-ocean ridge in an east-west direction and acts to separate the Greenland and Iceland Seas on its western side.

The Greenland Sea is about 3700m deep and located south of the Fram Strait. It is enclosed by the continental shelf of Greenland to the west, the mid-ocean ridge to the east, and the Jan Mayen Fracture Zone to the south. Equatorwards lies the close to 2200m deep Iceland Sea, bounded by the Icelandic continental shelf and the Denmark Strait to the south, the continental shelf of Greenland to the west, the Jan Mayen Fracture Zone to the north, and partly the mid-ocean ridge to the east. The Norwegian Sea is found east of the mid-ocean ridge and is defined by the Norwegian continental shelf to the east, the Greenland-Scotland Ridge to the south, the mid-ocean ridge to the west, and the entrance to the Barents Sea to the north. It is the deepest and largest area in the Nordic Seas, exceeding 3700m depth. The Norwegian Sea consists of two basins: the Norwegian Basin in the south and the Lofoten Basin in the north. Connected to the Norwegian Basin are the Faroese Channels, a channel network between the Faroe Islands and Shetland. The network consists of three distinguishable areas: the Faroe-Shetland Channel, the Wyville-Thomson Basin, and the Faroe-Bank Channel. The 1500-2000m deep Faroe-Shetland Channel east of the Faroe Islands connects to the Wyville-Thomson Basin, with the 450m deep Wyville-Thomson Ridge. Onward is the location of the Faroe-Bank Channel with a 850m deep sill, which leads to the North Atlantic Ocean.

1.3 Circulation

The deep circulation in the Nordic Seas is primarily dictated by the bathymetry, while the surface circulation is influenced by a warm poleward Atlantic inflow mainly on the eastern side of the region and a cold southward flow on the western side. The Atlantic water invades over the Greenland-Scotland Ridge, through the Denmark Strait, the Faroese Channels, and across the

Iceland-Faore Ridge. This water flows northwards following the Norwegian coast, where it is referred to as the Norwegian Atlantic Current. It carries much heat and salt from the North Atlantic to higher latitudes, and by providing salt acts as a density supplicant. Some of the water recirculates in the Norwegian Sea, while the rest is transported further north where the current splits. One branch enters the shallow Barents Sea on its way to the Arctic Ocean, while the other travels along the western slope of Spitsbergen as the West Spitsbergen Current. At the Fram Strait the Atlantic water either enters the Arctic Ocean or recirculates.

Transformed Atlantic water exits the Arctic Ocean through the deep Fram Strait, which is the only site enabling transfer of dense water between the Nordic Seas and the Arctic Ocean. Together with recirculating water off of the West Spitsbergen Current, this water flows southwards along the coast of Greenland as the East Greenland Current (EGC). The EGC is an important distributor of deep water in the Nordic Seas. At the Jan Mayen Fracture Zone, a branch splits off from the current and transports water masses into the Greenland Sea and is referred to as the Jan Mayen Current. Another branch is the East Icelandicic Current (EIC), found further south where it travels east along the North Icelandic slope and into the Norwegian Basin, supplying both the Iceland and Norwegian Seas [Macrander et al., 2014]. The remaining flow in the EGC travels toward the Denmark Strait to exit the Nordic Seas. A portion of the flow is too deep and forced southeast to escape through the deeper Faroese Channels [Macrander et al., 2014].

According to Wilkenskjeld and Quadfasel (2005), the water column in the Faroese Channels may be illustrated by a two-layered flow pattern: an inflow into the Norwegian Sea in the upper layer and an outflow into the North Atlantic Ocean in the lower layer. The Faroese outflow will henceforth refer to the deep water escaping through the channel network into the North Atlantic Ocean, where it contributes to the deep branch of the AMOC. These dense waters that manage to spill over the Greenland-Scotland Ridge are called overflows. The volume transport of these overflows are 3.2Sv ($1\text{Sv}=10^6\text{m}^3\text{s}^{-1}$) through the Denmark Strait, 1.9Sv through the Faroe Bank Channel, and approximately 1Sv over the Iceland-Faroe Ridge [Macrander et al., 2005; Jochumsen et al., 2017]. While the Denmark Strait transports most of the total overflow, the deeper Faroe Bank Channel is the primary passage for water from the Norwegian Sea to escape into the North Atlantic Ocean [Hansen and Østerhus, 2000].

The Nordic Seas is a region of both formation and modification of water, with multiple processes resulting in production of dense water. The traditional mechanism is the steady densification due to the surface water losing heat to the colder atmosphere at higher latitudes [Mauritzen, 1996]. As the temperature of the water decreases, the density increases and forces the water to sink to a depth where the surrounding water is of equal density [Østerhus et al., 2001]. This process is important regarding the inflowing warm Atlantic water as it circulates the Nordic Seas. Another dominant mechanism, especially considering the Iceland and Greenland Seas, is open-ocean convection [Rudels et al., 2005]. Open-ocean convection is a process in which the large bodies of water are transformed by periodic vertical mixing. A weakly stratified water column subjected to sufficient heat loss during winter causes density increase, with resulting dense water sinking [Marshall and Schott, 1999]. This process forms dense and nearly homogeneous water, where the intensity and duration of heat loss influences the convection depth and volume. A third mechanism for producing dense water is the haline convection: the injection of brine to the surface waters during ice formation. During the production of sea ice, salt is rejected from the freezing water and added to the surface waters. This raises the salinity of the surface waters, thus enhancing their density and forces the water to sink.

1.4 Water masses

A water mass is a parcel of water with properties determined by its origin and residence in the world ocean [Tomczak, 1999]. Due to circulation and mixing, any body of water may comprise various distinct water masses. To distinguish between the individual water masses we first made use of the hydrographical characteristics temperature, salinity, and density. Utilising a TS-diagram introduced by Helland-Hansen (1916), the mixing between water masses may be identified by the end points of mixing lines. Unfortunately, this method is limited to a composition of at most three water masses. However, Stefánsson (1968) established the use of chemical parameters such as nutrients and oxygen. Other chemical parameters include tracers such as chlorofluorocarbons (CFCs), which are gases released into the atmosphere during the 20th century [Walker et al., 2000]. Combining hydrographical and chemical parameters enabled a more detailed definition of the individual water masses and thus more ways to tell them apart.

The water in the Greenland Sea is affected by recirculating Atlantic water off of the West Spistbergen Current and invading waters from the Arctic Ocean, brought along with the East Greenland Current. Advection of Atlantic water has been especially important in this region, as it introduces surface waters with high salinities which are favourable for winter convection [Karstensen et al., 2005]. Through this process, the Greenland Sea used to be the an important producer of deep water in the Nordic Seas. However, tracer measurements imply that the deepest water has not been ventilated since the late 1970s [Karstensen et al., 2005]. Convection has instead been restricted to shallower depths (¡2000m), producing Greenland Sea Arctic Intermediate Water (GSAIW) with characteristics depending on the intensity and duration of winter. The GSAIW is distinguished as a cold and dense intermediate water mass, with high oxygen content. I define it within the density interval ($28.04 \leq \sigma_\theta \leq 28.06 \mathrm{kgm}^{-3}$). The Greenland Sea Deep Water (GSDW) is a product of previous strong convection with admixture of invading Arctic deep waters. It is in this study characterized by temperatures below θ=-1.07°C and salinities S≥34.9.

The intermediate water in the Iceland Sea is also formed by local wintertime convection and by mixing with advected water masses [Rudels et al., 2002]. This Iceland Sea Arctic Intermediate Water (ISAIW) is here identified as water colder than θ=0∘C and in the density interval $27.97 \leq \sigma_\theta \leq 28.01$kgm-3, with high oxygen content due to recent ventilation. The densest fractions of ISAIW in the Iceland Sea are produced on the northern rim of the gyre. There they are influenced by sea ice, enhanced atmospheric forcing, and an Atlantic inflow from the Norwegian Sea [Swift and Aagaard, 1981; Våge et al., 2015]. The deep water in the Iceland Sea was previously presumed to be the same or comparable to deep water found in the Norwegian Sea [Buch et al., 1996]. However, the Iceland Sea is influenced by the Arctic through the East Greenland Current, which provides saline waters. Therefore, observations of marginally higher salinities in addition to greater values of CFCs brought Fogelquist et al. (2003) to separate the Iceland Sea Deep Water (ISDW) and the NSDW. In this case, the ISDW is distinguished as water with temperatures $\theta \leq$-0.85°C and salinities S≥34.9. Another water mass originating from this region is the Modified East Icelandic Water (MEIW), which is formed on the North Icelandic Shelf during winter convection [Stefansson, 1962]. This water is defined by the intervals $1 \leq \theta \leq 3$°C and $34.7 \leq S \leq 34.9$ [Fogelqvist et al., 2003].

Warm Atlantic water enters the surface layers of the Norwegian Sea from the south. This water acts as a lid on the water column, preventing deep water production in this area. The intermediate and deep waters in the Norwegian Sea are therefore primarily influenced by water invading from neighbouring regions. Intermediate waters from the Iceland and Greenland Seas reach the Norwegian Sea by isopycnal spreading [Blindheim and Rey, 2004], flowing along lines of constant density. These waters form a layer of Norwegian Sea Arctic Intermediate Water

(NSAIW) beneath the warm Atlantic surface water [Blindheim, 1990]. The NSAIW is characterized as the salinity minimum layer within the Norwegian Sea (34.87≤S≤34.90) and is here restricted to the density layer $28.00 \leq \sigma_\theta \leq 28.04 \mathrm{kgm}^{-3}$. Aagaard et al. (1985) together with Swift and Koltermann (1988) established that the deeper part of the Norwegian Sea is a mixture of about equal portions of deep water from the Greenland Sea and Arctic Ocean. This Norwegian Sea Deep Water (NSDW) is in this case defined as water colder than θ=-0.9°C and with salinities centered around S=34.91.

Part of the North Atlantic Current invades the Nordic Seas across the Iceland-Faroe Ridge, close to the Faroese Channels. It is here named Modified North Atlantic Water (MNAW) and describes a water mass within the intervals $35.1 \leq S \leq 35.3$ and $7 \leq \theta \leq 8.5$°C [Hansen and Østerhus, 2000].

The deep outflow in the Faroese Channels is classically thought to be composed of NSDW, NSAIW, and MNAW [Borenäs and Lundberg, 1988; Turrell et al., 1999; Fogelqvist et al., 2003]. Previous studies have also mentioned MEIW [Borenäs and Lundberg, 1988; Hansen and Østerhus, 2000], which is brought along with the East Icelandic Current to the mouth of the Faroese Channels. Eldevik et al. (2009) proved that the outflow is also influenced by water passing through the Jan Mayen Channel, which connects the Greenland Sea and Norwegian Sea. Therefore water from any region in the Nordic Seas may influence the deep outflow in the Faroese Channels.

Chapter 2

Data and methods

2.1 Data

The data used in this thesis was obtained from the Global Ocean Data Analysis Project version 2 (GLODAPv2) data product, which consists of hydrochemical data from the Atlantic, Pacific, Southern, and Arctic Oceans (http://www.glodap.info) [Olsen et al., 2016]. The parameters extracted for use were potential temperature (θ), salinity (S), potential density (σ_θ), dissolved oxygen, the nutrients nitrate, silicate, and phosphate, and the chlorofluorocarbon CFC-12. These parameters have undergone comprehensive control of quality, leading to the accuracy of the individual parameters to be within 0.005 in salinity, 1% in oxygen, 2% for the nutrients, and 5% for the CFC-12. Data covering the Nordic Seas was evaluated for the time period 1982-2009. In addition, observational data from 2015 (with the EXPOCODE 58GS20150410) in the Faroese Channels was collected during the SNACS project, which was financed by the Research Council of Norway. These measurements have not undergone the same excessive quality control as the GLODAPv2 data.

2.2 Source regions

To determine the composition of the outflow through the Faroese Channels, source water regions must be defined. A source region is the location where a water mass is formed and obtains its specific properties [Tomczak, 1999]. The regions were selected on the assumption that their water masses could influence water in the Faroese Channels. The Faroese Channels are directly connected to the Norwegian Sea, which receive waters from both the Greenland and Iceland Seas. The East Icelandic Current transports water formed at the Icelandic shelf to the entrance of the Faorese Channels. Atlantic water invading over the Iceland-Faroe Ridge is also brought along with the flow to the mouth of the channel network. A box for each source region were located with centres at 67°N3°W for the Norwegian Sea, at 70°N14°W for the Iceland Sea, at 74.5°N4°W for the Greenland Sea, at 63°N8°W for the East Icelandic Current, and for the Iceland-Faroe Ridge at 63°N10°W (Fig.2.1). The source region for the Norwegian Sea was located in the Norwegian Basin, as this area is in direct contact with the Faroese Channels. The box in the Iceland Sea includes the northern border of the basin, where the densest and deepest convection takes place [Våge et al., 2015]. The source region on the Iceland-Faroe Ridge overlaps with the East Icelandic Current, but data from different years are examined in the two respective boxes. The observational data available from the Faroese Channels were split into two

regions; the Faroe-Shetland Channel with a centre at 60.5°N5°W and the Faroe Bank Channel at 61.5°N8.5°W.

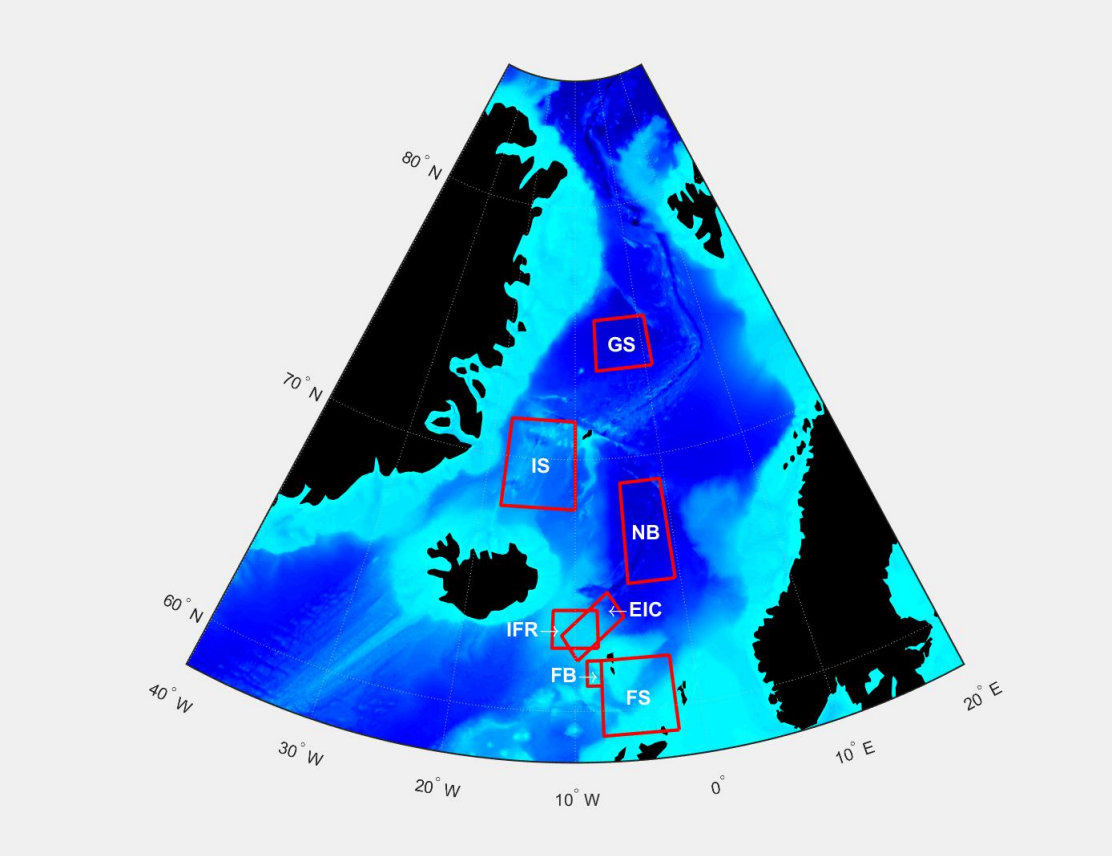

Figure 2.1: Map of the Nordic Seas with indicated source regions for the Greenland Sea (GS), Iceland Sea (IS), Norwegian Basin (NB), the Iceland-Faroe Ridge (IFR), and cross-section of the East Icelandic Current (EIC). The Faroe-Shetland Channel (FS) and the Faroe Bank Channel (FB) are also indicated.

Not all data within each source region was included in the analysis. There was only data available in the Faroese Channels during specific years (Fig.2.2). The first year with measurements taken in both the Faroe-Shetland and Faroe Bank Channel was 1997, which did not contain data of silicate. The next year with data was 2001, which omitted all nutrients. In 2002, there was observational data in both channels and corresponding measurements taken in the established source regions except for the East Icelandic Current (not shown). The East Icelandic Current region only contained data from 1992 and 1994, with no corresponding data in the Faroese Channels. There were no observations in the Norwegian Sea after 2002 included in GLODAPv2, while the Faroese Channels had data from both 2009 and 2015.

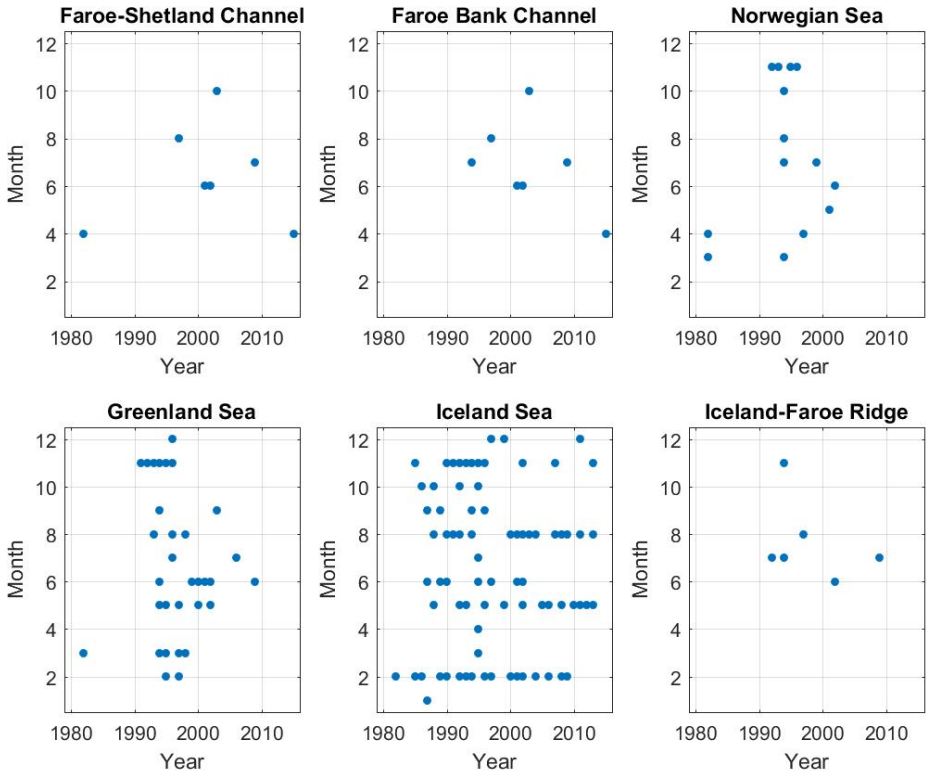

Figure 2.2: Annual and seasonal distribution of available data in the source regions, as well as the Faroese Channels.

2.3 Source waters

A water composition is a mixture of different water masses, for which a set of pure water masses must have been present before the mixing occurred. These water masses are referred to as source waters and reflects the properties of a water mass as it was formed in its source region, or in its pure form. From each source region either one or two source waters were defined. This was achieved by plotting the hydrochemical water properties against either depth or salinity, to inspect the structure of the water column as well as the correlation between the parameters. With available measurements in nearly all source regions in June 2002, source water descriptions were extracted from observational data at this specific time. Following the definition by Fogelqvist et al. (2003), the other water properties of MEIW were derived from July 1994. The detailed definitions of the source water masses which are to be used to determine the Faroese outflow composition are listed in Table 2.1, together with their standard deviation. The highest standard deviations are for the surface and intermediate waters while the lowest values are for the deep water, which is reasonable. Surface and intermediate waters are sensitive to atmospheric forcing and seasonal variation, while the more isolated deep waters conserve their properties.

The number of stations in source regions with measurements that fall within the respective source

Source waters	θ (°C)	Salinity	σ_θ	Oxygen (μmolkg^{-1})	Nitrate (μmolkg^{-1})	Phosphate (μmolkg^{-1})	Silicate (μmolkg^{-1})
MNAW	8.35 ±0.02	35.27 ±0.01	27.434 ±0.023	271±1	13.2±0.4	0.8±0.0	5.4±0.4
MEIW	1.78 ±0.81	34.81 ±0.01	27.840 ±0.052	311±4	13.1±0.1	1.0±0.0	6.5±0.2
ISAIW	-0.49 ±0.33	34.83 ±0.02	27.994 ±0.011	339±7	12.2±0.5	0.8±0.0	5.1±0.1
NSAIW	-0.17 ±0.27	34.89 ±0.00	28.026 ±0.014	305±1	14.1±0.2	0.9±0.0	7.3±0.5
GSAIW	-0.85 ±0.10	34.89 ±0.00	28.054 ±0.005	330±3	13.0±0.3	0.9±0.0	6.8±0.4
ISDW	-0.89 ±0.02	34.91 ±0.00	28.074 ±0.002	294±2	15.5±0.4	1.1±0.0	12.7±1.2
NSDW	-0.98 ±0.03	34.91 ±0.00	28.080 ±0.002	297±0	15.3±0.1	1.0±0.0	12.6±0.7
GSDW	-1.10 ±0.01	34.91 ±0.00	28.081 ±0.001	303±0	14.9±0.1	1.0±0.0	12.1±0.2

Table 2.1: Source water masses with parameter mean and standard deviation values extracted from observational data in June 2002 to be used for OMP analyses.

water definitions are shown in Table 2.2. Note the low amount of available data which has been used to define MEIW.

Source waters	MNAW	MEIW	ISAIW	NSAIW	GSAIW	ISDW	NSDW	GSDW
Number of stations	7	2	29	20	78	34	44	21

Table 2.2: Number of stations with data used to extract the respective source water definitions in June 2002.

2.4 OMP analysis

Tomczak (1981) enabled the determination of several water masses in a composition by using hydrochemical parameters for a more detailed definition of source waters. This was taken even further by Mackas et al. (1987), and the end product provided by Tomczak and Large (1989) was named the optimum multiparameter (OMP) analysis. This method identifies the individual water masses mixed in a water sample composition, in addition to determining the contribution of each water mass to the composition.

The classical OMP analysis assumes quasi-conservation of parameters; the properties of water masses are only influenced through mixing. If a parameter is considered conserved, it has no sources or sinks. Thus, the conservation of mass also holds. This makes it possible to establish the composition of a water sample through solving a linear set of equations [Tomczak and Large, 1989]. By defining the hydrochemical parameters of the source waters, the linear set of equations

used to resolve the water composition are established. By including an equation for conservation of mass, the system becomes over-determined. These equations make up the source water matrix G. The number of columns in the source matrix G is equivalent to the number of hydrochemical parameters used to define the different source waters, while the number of source waters included in the analysis is given by the rows. The system of linear equations may in short be written as

$$Gx - d = R \tag{2.1}$$

where G is the source water matrix, x is a vector yielding the water sample composition, d is a vector composed of the observational data, while the vector R contains the residuals. In full, the set of equations Gx-d=R is written:

$$x_1T_1 + x_2T_2 + x_3T_3 + x_4T_4 = T_{obs} + R_T \tag{2.2}$$

$$x_1S_1 + x_2S_2 + x_3S_3 + x_4S_4 = S_{obs} + R_S \tag{2.3}$$

$$x_1O_{2,1} + x_2O_{2,2} + x_3O_{2,3} + x_4O_{2,4} = O_{2,obs} + R_{O_2} \tag{2.4}$$

$$x_1PO_{4,1} + x_2PO_{4,2} + x_3PO_{4,3} + x_4PO_{4,4} = PO_{4,obs} + R_{PO_4} \tag{2.5}$$

$$x_1NO_{3,1} + x_2NO_{3,2} + x_3NO_{3,3} + x_4NO_{3,4} = NO_{3,obs} + R_{NO_3} \tag{2.6}$$

$$x_1SiO_{4,1} + x_2SiO_{4,2} + x_3SiO_{4,3} + x_4SiO_{4,4} = SiO_{4,obs} + R_{SiO_4} \tag{2.7}$$

$$x_1 + x_2 + x_3 + x_4 = 1 + R_\Sigma \tag{2.8}$$

where T_i, S_i, $O_{2,i}$, $PO_{4,i}$, $NO_{3,i}$, and $SiO_{4,i}$ represent the predefined parameters temperature, salinity, oxygen, phosphate, nitrate, and silicate of the denoted i water type, respectively. T_{obs}, S_{obs}, $O_{2,obs}$, $PO_{4,obs}$, $NO_{3,obs}$, and $SiO_{4,obs}$ stand for the observed values in a given water sample while R represents the residual of each parameter. The last row (Eq.2.8) is the equation for conservation of mass; the sum of all source water fractions should equal unity. All source water fractions in the OMP analysis are restricted to be non-negative, but this enables the sum of source water fractions to exceed unity which is not preferred. By varying the composition of source waters, the OMP analysis seeks a solution with minimal residuals.

The source water parameters are not inevitably of equal importance for the OMP analysis due to accuracy of measurement and environmental variability. Adopting the method by Tomczak and Large (1989), all parameters are given a weight using the equation:

$$W_j = \frac{\sigma_j^2}{\delta_{j,max}} \tag{2.9}$$

where σ_j is an indication of how well parameter j explains the variability in water mass, and δ_j max is parameter j's maximum variance [Leffanue and Tomczak, 2004]. In other words, a respective parameter's weight is calculated by dividing each parameter variance in the source water matrix G by the maximum variance in the source water region [Tanhua et al., 2005]. The standard deviation given in Table 1 is squared to find the respective parameter's variance.

The specific weight of each individual parameter represents its reliability, and parameters assigned high weights are expected to have the greatest influence on determining the source waters in the composition. However, weights for mass cannot be estimated this way and these are usually weighted equal to the highest weight found for the other parameters. Generally, the highest weights are assigned to salinity and temperature as they are considered most accurate. They are also more conserved, whereas biogeochemical parameters are influenced by biological activity. The weights used in this analysis are given in the Table 2.3, with the mass conservation weighted equal to the potential temperature.

Parameter	Weights
θ	29
Salinity	4
Oxygen	1
Nitrate	1
Phosphate	6
Silicate	2

Table 2.3: Weights of the different hydrochemical parameters used to describe source waters, which are to be used in the OMP analysis.

Another version of the OMP analysis addresses the issue that not all parameters necessarily is conserved, where nutrients and oxygen may be influenced by biogeochemical processes. This is achieved by including a relation defined by Redfield et al. (1963), known as the Redfield ratio. It is a relation between dissolved organic carbon, nitrogen, phosphorus, silicate and dissolved oxygen, based on the biological cycle of plankton. This analysis version is therefore referred to as the extended OMP analysis [Karstensen and Tomczak, 1998]. When incorporating waters from distant source regions, a quasi-conservation of the biochemical parameters may no longer be considered. As an example, the source waters MNAW, GSAIW, and GSDW were analysed using both classical and an extended OMPanalyses (Fig.2.3). The mass conservation residuals have a clear structure in the extended version, with near zero residuals for dense waters and increasing values for lighter waters. The classical version provides a more chaotic arrangement, with no part of the water column being well described. Since the extended analysis works better for the dense portion of the density interval, this will be the version employed in this thesis.

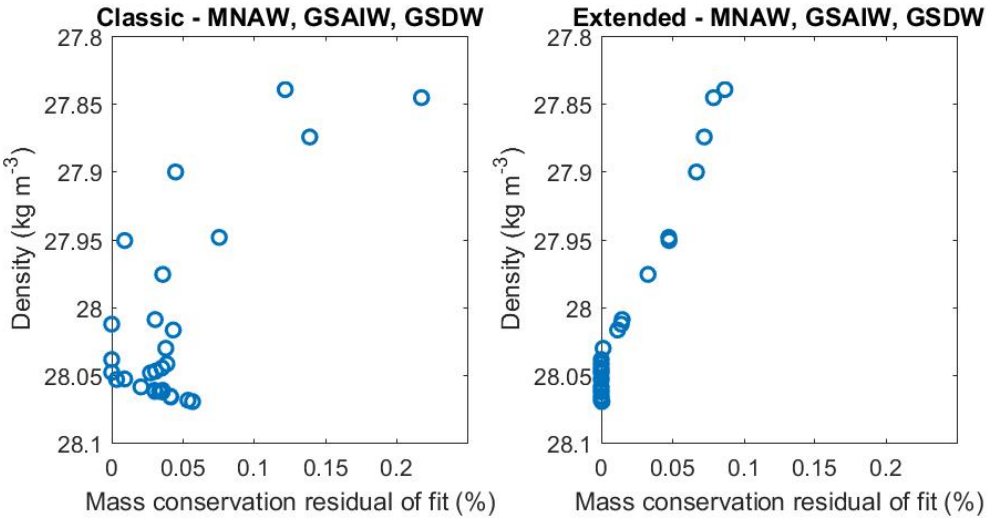

Figure 2.3: Mass conservation residual of fit vs. density of a) classical and b) extended OMP analyses of overflow water ($\sigma_\theta \geq 27.8 \mathrm{kgm}^{-3}$) composition in the Faroe-Shetland Channel in June 2002. Source waters MNAW, GSAIW, and GSDW were selected for the analyses.

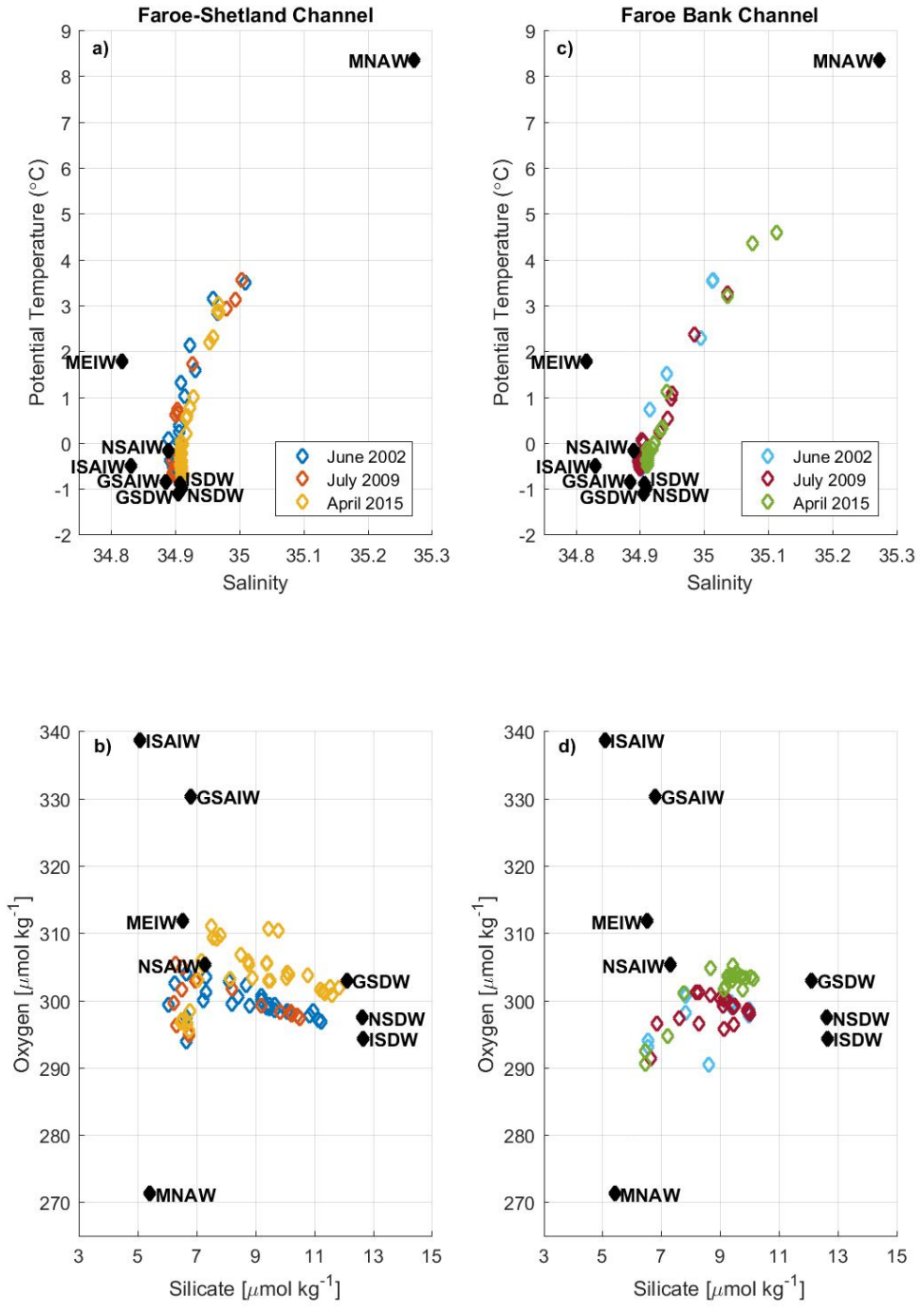

Figure 2.4: Mean values of source waters plotted in temperature against salinity and oxygen against silicate, together with observed data of outflow ($\sigma_\theta \geq 27.8 \mathrm{kgm}^{-3}$) in the Faroe-Shetland (a,b) and Faroe Bank Channel (c,d) for the three specific times June 2002 (dark/light blue), July 2009 (light/dark red), and April 2015 (yellow/green).

Some source waters are crucial to include in the OMP analysis of the Faroese outflow. To visualize which, the source waters mean values were plotted in the TS-space and oxygen-silicate parameter space together with the observed data in the Faroese Channels (Fig.2.4). The observed data extend down to temperatures and salinities of deep source waters; NSDW, ISDW, and GSDW. It curves up towards MNAW indicating the influence of another source water, else it would follow a straight mixing line between the Atlantic and deep water. MEIW appears to have a central position to encircle the observed data together with MNAW and a deep water mass. Looking at the oxygen-silicate parameter space, the data points bend clearly. Here there are many choices of source waters that would enclose the observed data points.

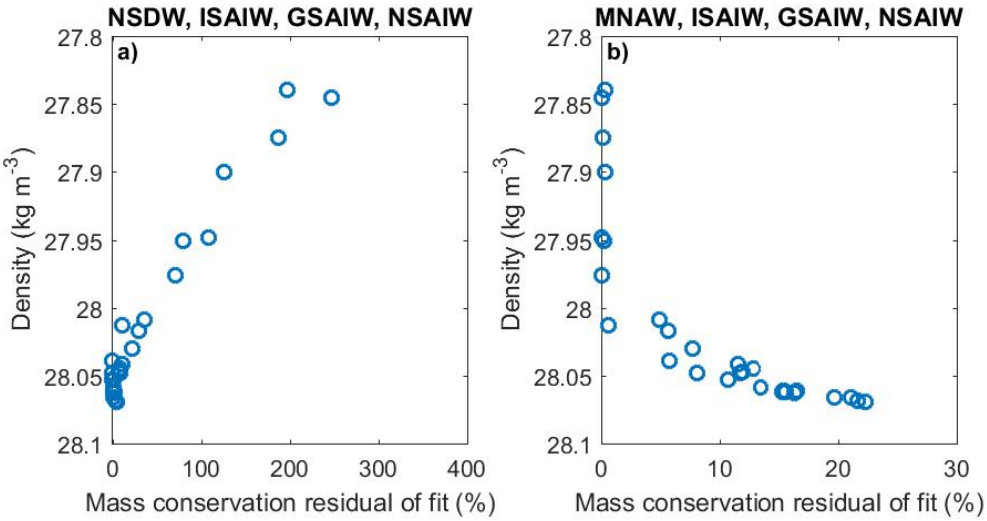

Figure 2.5: Mass conservation residual of fit vs. density of a classical OMP analysis of outflow ($\sigma_\theta \geq 27.8 \mathrm{kgm}^{-3}$) composition in the Faroe-Shetland Channel in June 2002. Source waters MNAW, ISAIW, GSAIW, and NSAIW were selected for the analysis in a) and NSDW, ISAIW, GSAIW, and NSAIW in b).

Two analyses excluding either all deep water or all Atlantic water were tested to confirm the argumentation above (Fig.2.5). Plotting the resulting mass conservation residual of fit against density provides information on what portion of water remains unexplained by the included source waters. Striving for as little residual as possible, the figure illustrate the necessity of both a deep and an Atlantic source. In Fig.2.5a the combination NSDW, ISAIW, GSAIW, and NSAIW excludes any Atlantic source water and produces extremely high residuals for densities $\sigma_\theta \leq 28.04 \mathrm{kgm}^{-3}$, with increasing residuals for decreasing densities. This highlights the need for a light source to be included to resolve all observational data in the analysis. In Fig.2.5b the deep water source has been omitted in the composition MNAW, ISAIW, GSAIW, and NSAIW. There are now residuals at high densities with a maximum for $\sigma_\theta = 28.07 \mathrm{kgm}^{-3}$, which decreases towards lighter densities to a minimum at $\sigma_\theta = 28.01 \mathrm{kgm}^{-3}$. This maximum is not found in Fig.2.5a where the deep water mass NSDW is included. A dense water source is thus needed to describe water exceeding this density. Inspecting the lighter waters above $\sigma_\theta \leq 28.01 \mathrm{kgm}^{-3}$, the residuals again increase with decreasing density. This implies that the Atlantic water source selected for the analysis does not alone describe the lighter portion of the overflow water. Noting the difference in scale for the mass conservation residual of fit between the two panels, the residuals for$\sigma_\theta \leq 28.01 \mathrm{kgm}^{-3}$ are much smaller when MNAW is included. From Fig.2.5 it is clear

that both an Atlantic and a deep water source need to be included in the analysis of the overflow water composition in the Faroese Channels.

An extended analysis was performed on water with densities considered deep enough to be part of the Faroese outflow; densities exceeding ($\sigma_\theta \geq 27.8 \text{kgm}^{-3}$). I included six parameters in the analysis (potential temperature, salinity, oxygen, nitrate, phosphate, and silicate), which together with mass conservation enables five source waters to be resolved at the same time. Every source water (Table 2.1) was included in the analysis at some point to test different combinations. With an interest in the latest potential variations in the Faroese outflow, all available data with values for the six parameters in the Faroese Channels for June 2002, July 2009, and April 2015 were used for the analysis. The source water definitions were kept the same, with characteristics extracted from source regions in June 2002 and for MEIW in July 1994. The outflow composition was analysed for both the Faroe-Shetland Channel and the Faroe Bank Channel to investigate the composition stability within the channel.

A reasonable starting point for the OMP analysis would be to include the water masses most likely to be found in the Faroese Channels as they are produced in the near vicinity; NSDW, NSAIW, MEIW, and MNAW. When a satisfactory outflow composition in the Faroese Channels for June 2002 have been determined, the same source water combination will be used to resolve the compositions for July 2009 and April 2015. Temporal variations in the outflow will then be indicated by changes in mass conservation residuals, vertical source water distribution, and source water fractions. A concern is the effect of seasonal variation on the outflow composition, introducing uncertainties to the results. Such a variation would most likely be found at the interface of the outflow, where the it interacts with water masses lying above. By separating the outflow into three density layers, the differences between the lightest and denser layers may be examined.

A general overview of the water properties in the Faroese Channels will be presented first, to gain a better understanding of the dynamics in the channel network. Possible trends in different hydrochemical parameters will provide further insight of the potential variation in the Faroese outflow. After establishing the outflow composition, a comparison of the source water fractions at the three specific times June 2002, July 2009, and April 2015 will indicate any temporal evolutions in the Faroese outflow.

2.5 Uncertainties in OMP analysis

The errors in the OMP analysis are linked to uncertainties in data measurement, seasonal and interannual variability, and source water definitions. Since data extracted from GLODAPv2 have undergone comprehensive quality control, the accuracy of the individual parameters are high and introduce small uncertainties. On the other hand, data provided by the SNACS project contain higher uncertainties due to less thorough quality control. The definitions of time-dependet source waters introduce errors, where seasonal and interannual variability contribute. These uncertainties are considered when assigning parameter weights.

The number of hydrochemical parameters included in the OMP analysis determines how many water masses which can be resolved. This denies the possibility to include all observed water masses in the analysis, so only the water masses most likely to be found at the location of interest should be included. Excluding an influential source water in the analysis would produce a flawed outflow composition, where the density range of a missing source water is indicated by mass conservation residuals. These represent the divergence between the calculated and observed composition [Tanhua et al., 2005]. Since the analysis uses a set of predefined source waters, it does not take into account any temporal changes in their characteristics. Thus, any high mass

conservation residuals may serve to identify periods of abnormal source water characteristics, but does not reveal which changes the source waters have undergone [Leffanue and Tomczak, 2004]. This might call for a redefinition or addition of source waters to composition.

Setting the criteria that mass conservation residuals must not exceed 5% regulates the uncertainties which we allow to be included in the analysis. However, different source water combinations can still produce a solution which satisfies the residual criteria, where some combinations prove physically unreasonable. An objective examination is needed to determine if the analysis results are realistic.

Disagreements on the true Redfield ratio also introduce uncertainties when employing an extended OMP analysis. All results presented in this thesis meet the residual criteria ¡5%, often with considerably low values.

Chapter 3

Results

3.1 Water property variations in the Faroese Channels

A general understanding of the Faroese Channels may be achieved by examining the water column structure and its temporal variation. Here I consider the months of June 2002, July 2009, and April 2015. The distribution of the temperatures and salinities in the Faroe-Shetland Channel illustrates a strongly stratified water column with warm, saline water at the surface and cold, fresh water at the bottom (Fig.3.1). The interface of the deep outflow in the channels is marked by the σ_θ=27.8kgm^{-3} isopycnal, which slopes from the northwest down to the southeast side of the channel in June 2002 and July 2009. The isopycnals slope due to the shear in the flow through the channel, with an inflow at the surface and an outflow in the deep interior. This shear is indicated by the steep temperature and salinity gradients. More horizontal gradients in 2009 result in a less steep isopycnal. The corresponding isopycnal in April 2015 is rather flat. However, this section is located closer to the mouth of the channel, where the circulation within the channel is not as pronounced.

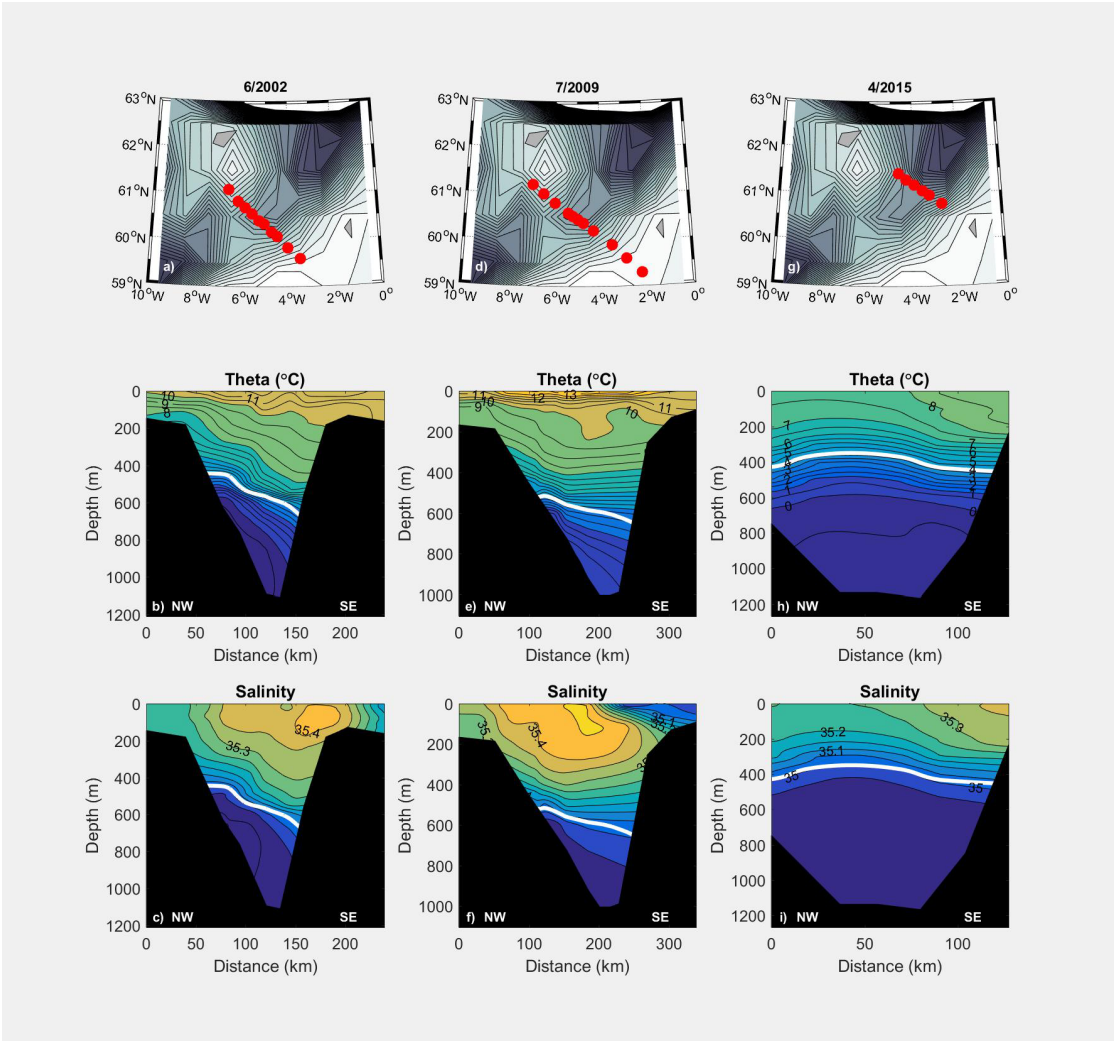

Figure 3.1: Maps showing transects taken in the Faroe-Shetland Channel (a,d,g) together with vertical sections of water properties with depth in June 2002 (a-c), July 2009 (d-f), and April 2015 (g-i). The white line indicates the σ_θ=27.8kgm^{-3} isopycnal, marking the interface of the outflow water. The endpoints of the sections are indicated by the directions northwest (NW) and southeast (SE), where the Faroese Islands are located on the northwestern and Shetland on the southeastern sides.

When comparing the water property profiles of the three time periods the largest discrepancy is found for April 2015, with both decreased temperatures and salinities above 400m. Surface temperatures are correlated to seasonality, with decreased temperatures during winter and spring caused by a larger heat loss to the colder atmosphere. The surface temperatures in April 2015 is therefore naturally lower compared to the summer in 2002 and 2009. The section taken in April 2015 is in addition taken closer to the mouth of the Faroe-Shetland Channel before much recirculation within in the channel may take place and it is deeper which enables a larger portion of dense water to enter. All of these factors may contribute to the differences between the vertical transects of 2002/2009 and 2015. The water masses above 400m in June 2002 and July 2009

are similar, with slightly higher values in July 2009. The temperature in the overflow range vary from -0.5°C to 4°C with salinities 34.90-35.05 in all three transects. The σ_θ=27.8kgm^{-3} isopycnal in April 2015 is located at about 400m depth, while it is found around 450-700m in June 2002 and 500-650m in July 2009. While it appears to be a larger volume of deep water in April 2015, this section is placed closer to the mouth of the channel where little recirculation has occurred yet. The difference in depth between 2002 and 2009 could indicate a variation in volume flux.

Inspecting the biogeochemical properties of the water column the maximum amounts of silicate are found in the outflow, while the values decrease towards the surface of the channel (Fig.3.2). Water located at 0-200m depth may contain little nutrients due to biological activity, while deep and old water has had time to accumulate high amounts from sinking particles and remineralization [Sarmiento, 2013]. This is the case for June 2002 and July 2009. The amount of silicate in April 2015 at the surface is larger. Nutrient contents are heavily utilized during the spring bloom primary production, suggesting that the transect in April was taken before the onset. There was a decrease in the silicate content of the outflow between June 2002 and July 2009, but the transect in 2009 is shallower which would inhibit the presence of denser water with high silicate content. Values in April 2015 are similar to June 2002. The amount of oxygen increases with depth, with a core of minimum values at 100m depth on the southeastern slope for both June 2002 and July 2009. The solubility of oxygen in water is mainly controlled by the temperature of the water, where high temperatures correspond to low oxygen content. High temperatures are found at the southeastern slope for both 2002 and 2009. The amount of oxygen in the channel in April 2015 is considerable, correlating to the general low temperatures of the water column. There is a layer with exceptionally high CFC-12 content at 400-600m depth during this time period, with decreasing values below. Due to increasing atmospheric CFC-12 content until around year 2000, the ocean content of CFC-12 is still equilibrating with the air. A recently ventilated water mass would be in balance with the atmospheric CFC-12, while a water mass which has not been at the surface for some time would be undersaturated and increase its content upon contact with the atmosphere. The minimum amounts of CFC-12 are found at the bottom for June 2002 and July 2009, where there is deep water which has not been recently ventilated. Fogelqvist et al. (2003) estimated that NSDW was last in contact with the atmosphere 30 years ago, while ISDW came close behind with an age of about 25 years. Maximums are found on the northwestern slope at 400m and 600m depth for 2002 and 2009, respectively. The CFC-12 content in April 2015 is high.

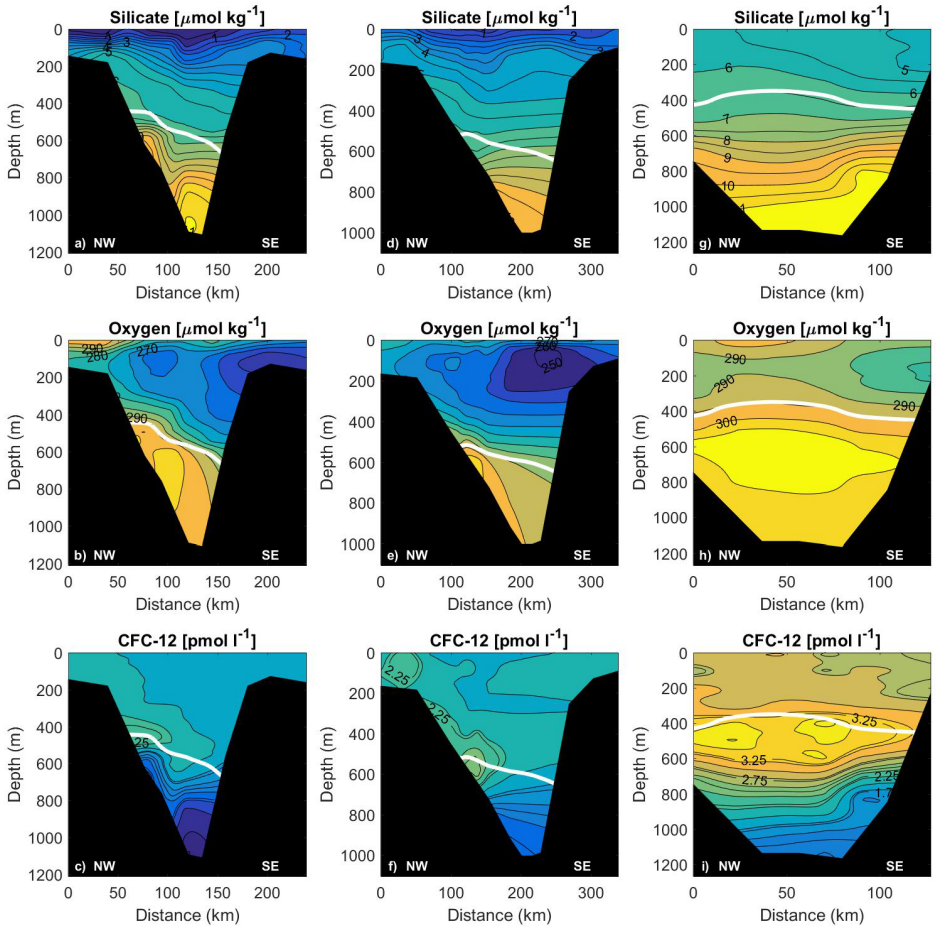

Figure 3.2: Vertical sections of water properties in the Faroe-Shetland Channel in June 2002 (a-c), July 2009 (d-f), and April 2015 (g-i). The white line indicates the σ_θ=27.8kgm^{-3} isopycnal, marking the interface of the outflow water. The endpoints of the sections are indicated by the directions northwest (NW) and southeast (SE), where the Faroese Islands are located on the northwestern and Shetland on the southeastern sides.

The Faroe Bank Channel is shallower than the Faroe-Shetland Channel, thus the stratified structure of the water column is compressed and some of the denser water is forced to recirculate. Due to different Atlantic sources, the surfaces of the Faroe Bank and Faroe-Shetland Channels are dissimilar. The inflow influencing the Faroe Bank Channel enters over the sill, while another branch flows over the Wyville-Thomson Ridge and directly into the Faroe-Shetland Channel.

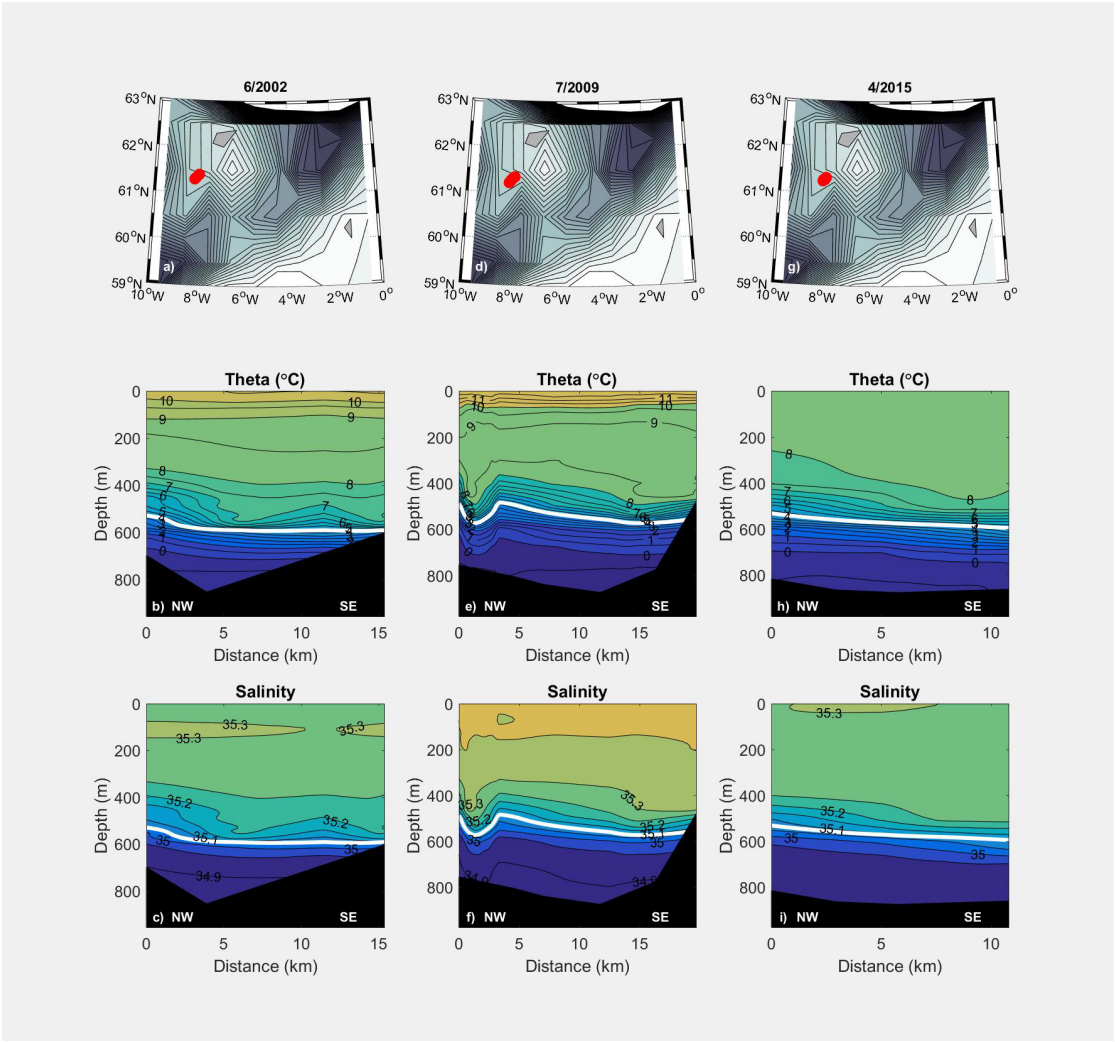

Figure 3.3: Maps showing transects taken in the Faroe Bank Channel (a,d,g) together with vertical sections of water properties with depth in June 2002 (a-c), July 2009 (d-f), and April 2015 (g-i). The white line indicates theσ_θ=27.8kgm^{-3} isopycnal, marking the interface of the outflow water. The endpoints of the sections are indicated by the directions northwest (NW) and southeast (SE), where the Faroese Islands are located on the northwestern and Shetland on the southeastern sides.

As seen in Fig.3.3 the deep outflow in the Faroe Bank Channel has the hydrographical properties of -0.5≤θ≤4°C and 34.90≤S≤35.05, which are stable over the years and identical to the outflow upstream. Due to the temporal uniform outflow, the σ_θ=27.8kgm^{-3} isopycnal is found at the same depth of about 550m during all three time periods sloping slightly. The upper 200m of the channel contains the maximum temperatures and salinities, which are largest in July 2009. There was no temperature gradient in the upper 100m of the water column in April 2015 compared to the two other years, which is due to the difference in season where the highest temperatures are found during summer. Between 200m and 400m there is a rather uniform layer, likely a result of mixing in the channel. This layer is also seen in the chemical properties of the

outflow, especially when examining the oxygen values (Fig.3.4). The mixed layer contained some lower oxygen values in July 2009 compared to June 2002, while the whole water column has seen an increase in April 2015. These oxygen variations were the same in the Faroe-Shetland Channel. The silicate content appears the same for the time periods when considering the effect of biological activity, while the amount of CFC-12 steadily increases between the years.

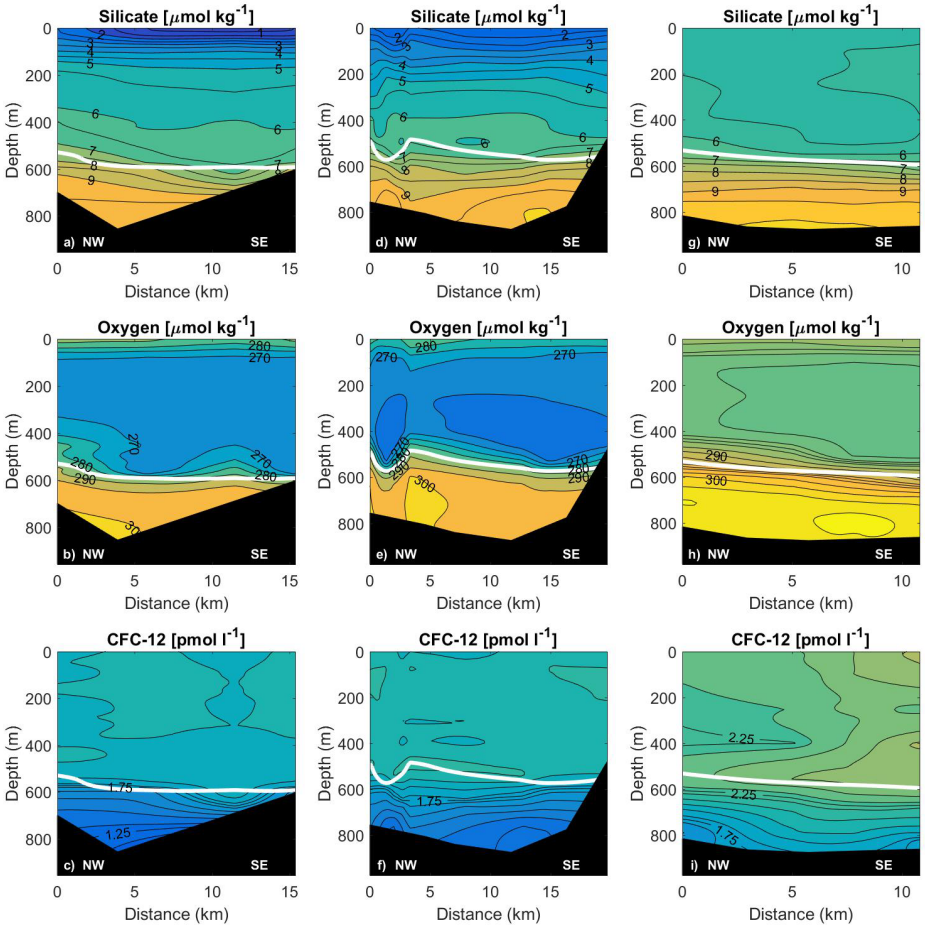

Figure 3.4: Vertical sections of water properties with depth in the Faroe Bank Channel in June 2002 (a-c), July 2009 (d-f), and April 2015 (g-i). The white line indicates the σ_θ=27.8kgm^{-3} isopycnal, marking the interface of the outflow water. The endpoints of the sections are indicated by the directions northwest (NW) and southeast (SE), where the Faroese Islands are located on the northwestern and Shetland on the southeastern sides.

3.2 Temporal evolution of outflow properties

A clearer view of possible trends in the outflow is provided by separating its density range into the three layers $27.80 \leq \sigma_\theta < 28.01 \text{kgm}^{-3}$, $28.01 \leq \sigma_\theta < 28.04 \text{kgm}^{-3}$, and $\sigma_\theta \geq 28.04 \text{kgm}^{-3}$ (Fig.3.5**??**). The first observation of the densest layer$\sigma_\theta \geq 28.04 \text{kgm}^{-3}$ was in 1997, implying that no water of this density was present in the channel before this. However, the only years containing data before 1997 are 1982 in the Faroe-Shetland Channel and 1994 in the Faroe Bank Channel. In addition to sparse data, observations show considerable short-term variations of water properties [Fogelqvist et al., 2003]. Thus, water with density$\sigma_\theta \geq 28.04 \text{kgm}^{-3}$ may have been present in the channels before 1997, but is not captured in the available data.

Generally the densest layer was the most stable in the channels, while the opposite held for the lightest layer which is more susceptible to be influenced by overlying water masses. This was also indicated by the large error bars for the temperature, salinity, and oxygen values in the lightest density layer. In the Faroe-Shetland Channel (Fig.3.5), the temperatures of the different density layers appear nearly constant with time, except for a decrease of 1°C in 1997 for the lightest portion of the outflow. Since the observational data before 1997 are sparse it is hard to tell if the decrease has taken place over time or if it is a special occurrence for this specific year. For the same density interval there was also a dip in salinity in 1997 by 0.05. Afterwards, salinities steadily increased in the consecutive years with data. The salinity has overall increased by 0.02 over the time period 1982-2015. The values in the densest layer decreased by 0.005 in 1997-2009 before increasing by 0.01 from 2009 to 2015. The same increase is seen in the middle density interval, which previously fluctuated around 34.895. However, these trends may be just fluctuations since no trend analysis was performed for validation. On the other hand, the temporal evolution is based on yearly mean values which could provide some indication of trends in properties.

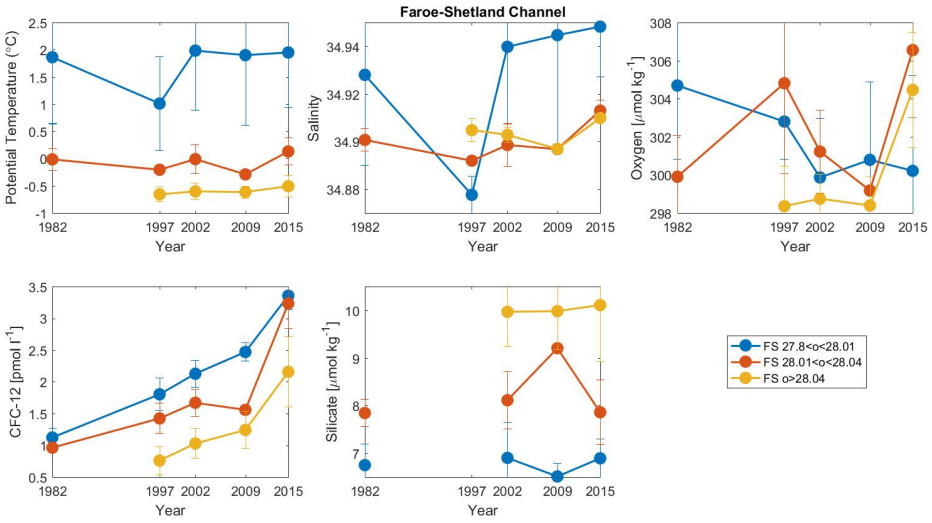

Figure 3.5: Mean values and their standard deviations for hydrochemical properties of the three outflow density layers $27.80 \leq \sigma_\theta < 28.01 \text{kgm}^{-3}$ (blue data), $28.01 \leq \sigma_\theta < 28.04 \text{kgm}^{-3}$ (red data), and $\sigma_\theta \geq 28.04 \text{kgm}^{-3}$ (yellow data) in the Faroe-Shetland Channel during the time period 1982-2015.

The amount of oxygen contained within a water mass also depends on how recently it has been ventilated. Since deep waters generally have a lower oxygen content than intermediate water, the variations of oxygen content in the outflow may indicate the presence of different water masses or interchanging influence by source waters. The mean oxygen content of the lighter outflow decreased over the 30 years. The middle layer had a rise in 1997 before decreasing over the next 12 years, to be followed by a similar spike in 2015. A parallel increase in 2015 is seen for the densest interval, which appear stable before this. Similar values and behavior of the densest and middle layer may indicate a homogenization of the two. Temporal evolution of CFC-12 mean values indicate a positive trend for the overall outflow, with the general largest increase of CFC-12 from 2009 to 2015. There is a 20 year gap in the silicate data so there is no distinguishable trends. There is a rise for the middle density interval in 2009 and together with a minimum in oxygen content, could indicate an increased influence of deep water.

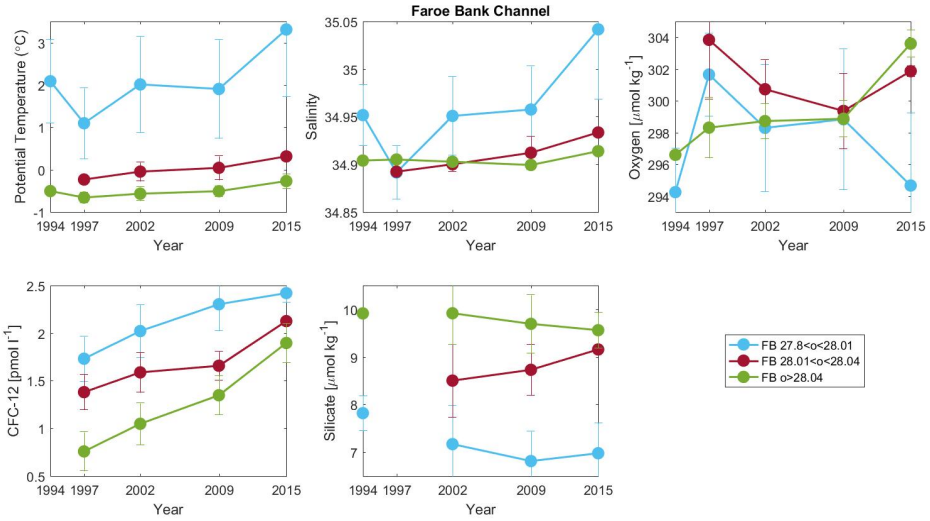

Figure 3.6: Mean values and their standard deviations for hydrochemical properties of the three outflow density layers $27.80 \leq \sigma_\theta$¡$28.01 \mathrm{kgm}^{-3}$ (blue data), $28.01 \leq \sigma_\theta$¡$28.04 \mathrm{kgm}^{-3}$ (red data), and $\sigma_\theta \geq 28.04 \mathrm{kgm}^{-3}$ (green data) in the Faroe Bank Channel during the time period 1982-2015.

Generally in the Faroe Bank Channel the temperature and salinity increased over the time period 1997-2015 (Fig.**??**). The lightest density interval saw a considerable increase from 2009 to 2015 in both. This indicates an increased influence of Atlantic water in this portion of the outflow, and likely due to different Atlantic sources this change was not reflected in the Faroe-Shetland Channel. However, there was a similar dip in temperature and salinity in the lightest layer in 1997 at both locations. The two densest layers saw an increase in oxygen content from 2009 to 2015 similar to the Faroe-Shetland Channel, but smaller. The lightest layer decreased over the time period 1997-2015, which was the same as observed upstream. The oxygen values in 2009 were similar in the three layers. There was a trend of increasing CFC-12 in the outflow for all three density layers, but the overall content was smaller compared to the Faroe-Shetland Channel. In 1997 the data did not include silicate, but from 2002 to 2015 the amount increased in the middle density interval while it decreased in the two other intervals. Similar behavior and parameter values growing closer towards the end of the time period suggests homogenization

between the two denser layers. Similar trends in the Faroe-Shetland and Faroe Bank Channel validate that some water found upstream finds its way towards the sill instead of recirculating or outflowing the Wyville-Thomson Ridge.

3.3 Source waters contributing to outflow in June 2002

The initial analysis was run with the source waters in closest proximity of the Faroese Channels: MNAW, MEIW, NSAIW, and NSDW (Fig.3.7). The mixing lines between the four include all observational data within their spanned parameter space in the TS-diagram, and nearly all are included when looking at oxygen and silicate as well. This is reflected in the mass conservation, where there is almost no residual for densities exceedingσ_θ=28kgm^{-3}.There is some residual forσ_θ=28.04kgm^{-3} and increasing residuals for $\sigma_\theta \leq$28.01kgm^{-3}. For all observational data to be contained in the spanned parameter space by oxygen and silicate values, an additional source water must be included in the analysis.

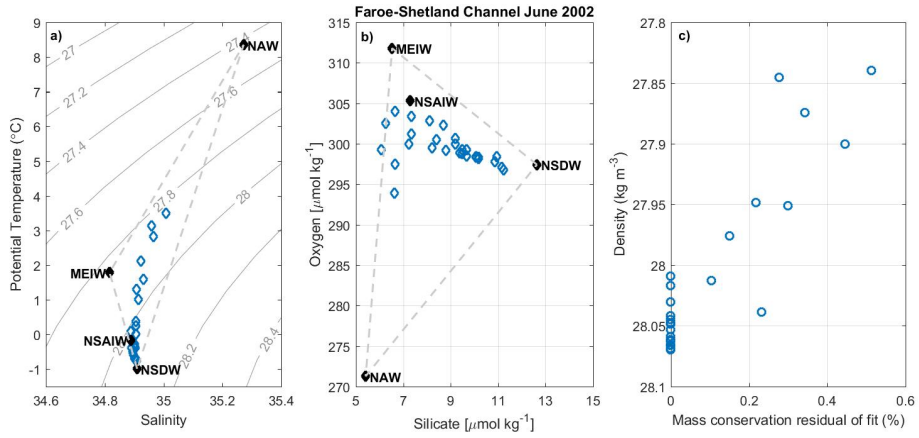

Figure 3.7: The observed data (blue diamonds) of outflow water ($\sigma_\theta \geq$27.8kgm^{-3}) in the Faroe-Shetland Channel in June 2002 plotted in salinity against potential temperature in a) with isopycnals (gray lines) and mixing lines (gray dashed lines), and in silicate against oxygen in b) including mixing lines. The mean values for the source waters MNAW, MEIW, NSDW, and NSAIW (black diamonds) are indicated. The resulting mass conservation residual of fit vs. density of an extended OMP analysis is shown in c).

Both ISAIW and GSAIW include more of the observed data in their spanned parameter space (Fig.3.8). The mass conservation residuals in the density range 28.01kgm-3 improve, with lower values. However, the residuals in the remaining layer deteriorates, especially for the density interval 28.04$\leq\sigma_\theta\leq$28.06kgm^{-3}. The two different source water combinations produce a similar pattern of residuals, but the GSAIW give some higher values at densities in the intervals 28.04$\leq\sigma_\theta\leq$28.06kgm^{-3} and $\sigma_\theta\leq$28.01kgm^{-3}. This suggests that a combination including ISAIW is preferred over GSAIW. Mass conservation residuals with ISAIW indicate that a source water describing the water in the density range 28.04$\leq\sigma_\theta\leq$28.06kgm^{-3} is missing from the composition. For the OMP analysis to be able to resolve the source water matrix the maximum number of source waters to include have already been reached. After having tested different source water combinations, NSAIW proved to be causing the increased residuals atσ_θ=28.04kgm^{-3}.

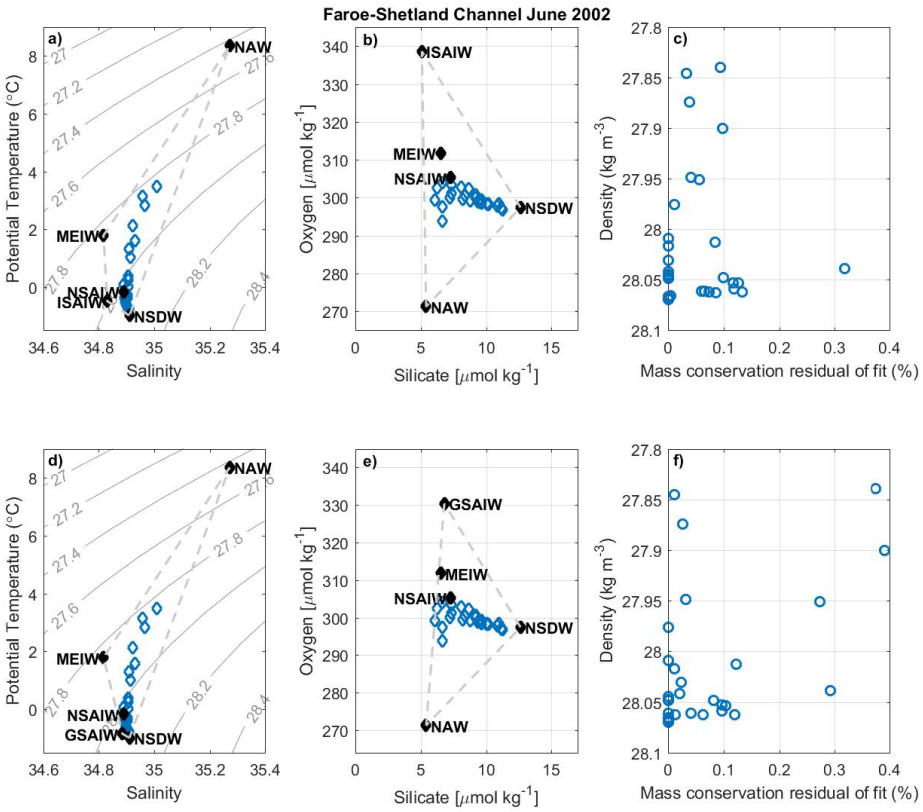

Figure 3.8: The observed data (blue diamonds) of outflow water ($\sigma_\theta \geq 27.8 \mathrm{kgm}^{-3}$) in the Faroe-Shetland Channel in June 2002 plotted in salinity against potential temperature in a) and d) with isopycnals (gray lines) and mixing lines (gray dashed lines), and in silicate against oxygen in b) and e) including mixing lines. The mean values for the source waters MNAW, MEIW, NSDW, ISAIW, GSAIW, and NSAIW (black diamonds) are indicated. The resulting mass conservation residual of fit vs. density of the extended OMP analyses are shown in c) and f).

Since NSAIW is influenced by ISAIW and GSAIW [Blindheim, 1990; Jeansson and Jutterström, 2017], exchanging it for the two seems reasonable. OMP analyses were also performed with either ISAIW or GSAIW, but the source water combination with GSAIW yielded negative mass conservation residuals which is a mathematically unsatisfied solution. Results for the combinations ISAIW together with GSAIW and only ISAIW are displayed in Fig.3.9. The combination with ISAIW and GSAIW gave low residuals, but little water of the outflow is fully explained by this solution of source waters. Only including ISAIW produced near zero residuals over the whole density layer, with the highest value of 0.01% at density σ_θ=27.84kgm^{-3}.

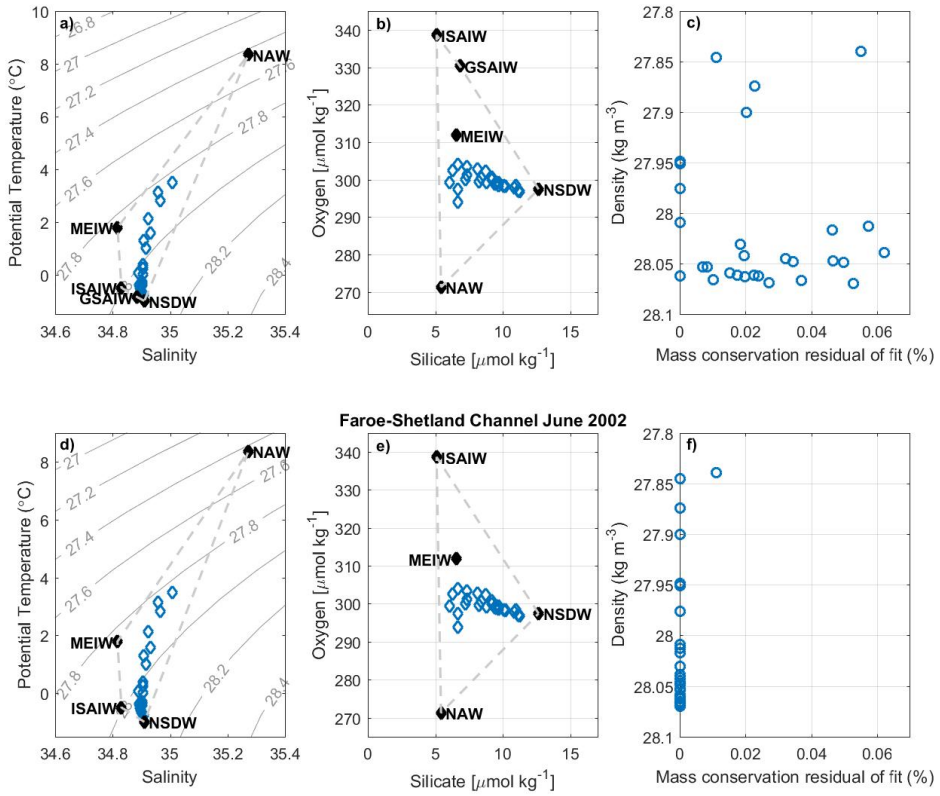

Figure 3.9: The observed data (blue diamonds) of outflow water ($\sigma_\theta \geq 27.8 \mathrm{kgm}^{-3}$) in the Faroe-Shetland Channel in June 2002 plotted in salinity against potential temperature in a) and d) with isopycnals (gray lines) and mixing lines (gray dashed lines), and in silicate against oxygen in b) and e) including mixing lines. The mean values for the source waters MNAW, MEIW, NSDW, ISAIW, and GSAIW (black diamonds) are indicated. The resulting mass conservation residual of fit vs. density of the extended OMP analyses are shown in c) and f).

It is reasonable to assume that waters originating from the Norwegian Sea may be found in the Faorese Channels since they are adjoining regions. By excluding these waters from the analysis, however, another outflow composition may be discovered consisting of waters from distant source regions. Provided there is no difference analytically between the two compositions, it is more realistic finding Norwegian water in the channel. If the remote source waters yield better results on the other hand, the composition of the outflow is up for discussion.

Three source water combinations were tested which should replace NSDW; intermediate water from the Iceland Sea together with either deep water from the same region or from the Greenland Sea, as well as intermediate and deep water from the Greenland Sea. Since NSDW is influenced by water found in the Greenland Sea [Aagaard et al., 1985; Swift and Koltermann, 1988; Blindheim and Rey, 2004], the latter alternative was included even though intermediate water from the Iceland Sea shows better prospects. The three combinations of source waters spans similar TS-spaces (Fig.3.10). With silicate against oxygen, all data points are encircled

when including ISDW while some fall outside when selecting GSDW. When selecting water from the Iceland Sea the mass conservation residuals increase for densities exceedingσ_θ=28.05kgm^{-3}, indicating that this water is not fully described by deep water originating from the Iceland Sea. Including intermediate and deep water from the Greenland Sea, there are some residuals for lighter densities than σ_θ=28.06kgm^{-3}. The best option appears to be the source water combination with intermediate water from the Iceland Sea and deep water from the Greenland Sea. Even though this solution does not include all observed silicate and oxygen data in the spanned parameter space, the mass conservation residuals are the lowest of the three combinations.

Adding GSAIW with a density range 28.04≤σ_θ≤28.06kgm^{-3} to the source water combination with Greenland Sea deep water and Iceland Sea intermediate water is unnecessary, since the water with these densities are mostly explained. A test run produced higher mass conservation residuals.

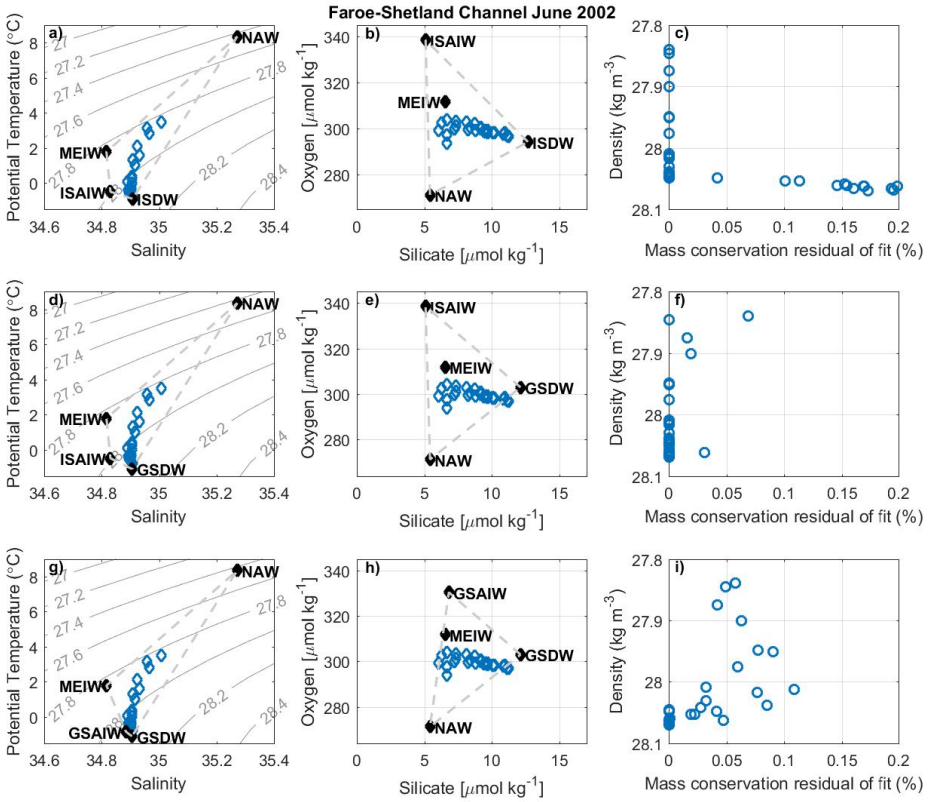

Figure 3.10: The observed data (blue diamonds) of outflow water (σ_θ≥27.8kgm^{-3}) in the Faroe-Shetland Channel in June 2002 plotted in salinity against potential temperature in a), d), and g) with isopycnals (gray lines) and mixing lines (gray dashed lines), and in silicate against oxygen in b), e), and h) including mixing lines. The mean values for the source waters MNAW, MEIW, ISAIW, GSAIW, ISDW, and GSDW (black diamonds) are indicated. The resulting mass conservation residual of fit vs. density of the extended OMP analyses are shown in c), f), and i).

The two best source water solutions of the Faroe-Shetland outflow are MNAW, MEIW, and

ISAIW, together with either NSDW or GSDW. A comparison between the mass conservation residuals of the two combinations reveal lower values for NSDW. To find NSDW in the Faroese Channels is more realistic as well since the channel network is connected to the Norwegian Sea, while the Greenland Sea is a more distant region. Thus, the source water solution of the deep outflow in the Faroe-Shetland Channel in June 2002 consists of MNAW, MEIW, ISAIW, and NSDW.

The Faroe Bank Channel is located downstream of the Faroe-Shetland Channel when following the direction of outflow. The source waters of the outflow upstream are expected to be found downstream. Since the Faroe Bank channel is shallower, some of the deeper water may recirculate between the two locations. This could produce dissimilarities between the two locations. Performing an analysis on the observed data in Faroe Bank Channel with the source water combination MNAW, MEIW, ISAIW, and NSDW found in the Faroe-Shetland Channel produced the results in Fig.3.11. The mixing lines in both property-diagrams enclose all data points and corresponding the mass conservation residuals are low. Thus, this source water composition also applies well for the Faroe Bank Channel outflow in June 2002.

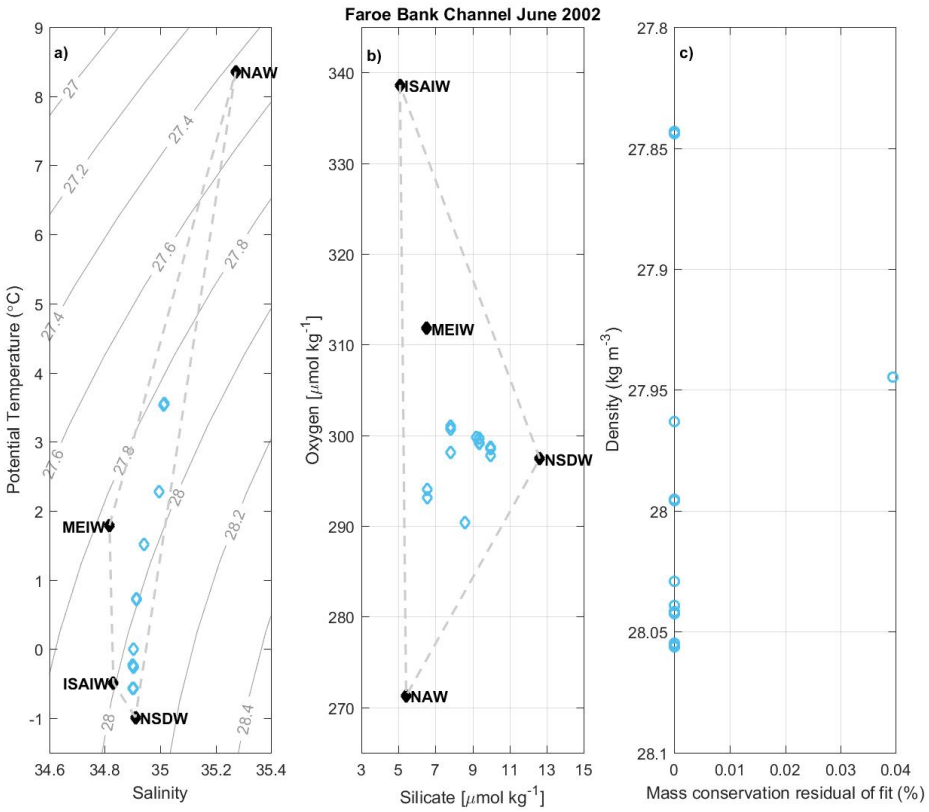

Figure 3.11: The observed data (blue diamonds) of outflow water ($\sigma_\theta \geq 27.8 \mathrm{kgm}^{-3}$) in the Faroe Bank Channel in June 2002 plotted in salinity against potential temperature in a) with isopycnals (gray lines) and mixing lines (gray dashed lines), and in silicate against oxygen in b) including mixing lines. The mean values for the source waters MNAW, MEIW, ISAIW, and NSDW (black diamonds) are indicated. The resulting mass conservation residual of fit vs. density of the extended OMP analysis is shown in c).

3.4 Temporal variation in overflow composition

Having determined the composition of the outflow in June 2002, it is time to investigate its temporal evolution by analysing the outflows in July 2009 and April 2015 using the same source water solution. The same definitions of the source waters derived from 2002 are used for the further analyses. Any increase in mass conservation residuals will indicate changes in source water properties or composition.

The results from the OMP analyses of the outflow in the Faroese Channels in July 2009 are shown in Fig.3.12. The observational data is similar to the observations from June 2002, and is located within the mixing lines between the source waters in both property-diagrams. The resulting mass conservation residuals are even lower than in 2002, for both the Faroe-Shetland and Faroe Bank Channels. Notice that ISAIW is not included in the source water solution for the Faroe Bank outflow, since this produced negative mass conservation residuals. It appears

the observational data can be described using only the three remaining source waters. The same source water combination found for the Faroese outflow in June 2002 is still a nice fit for the outflow in July 2009.

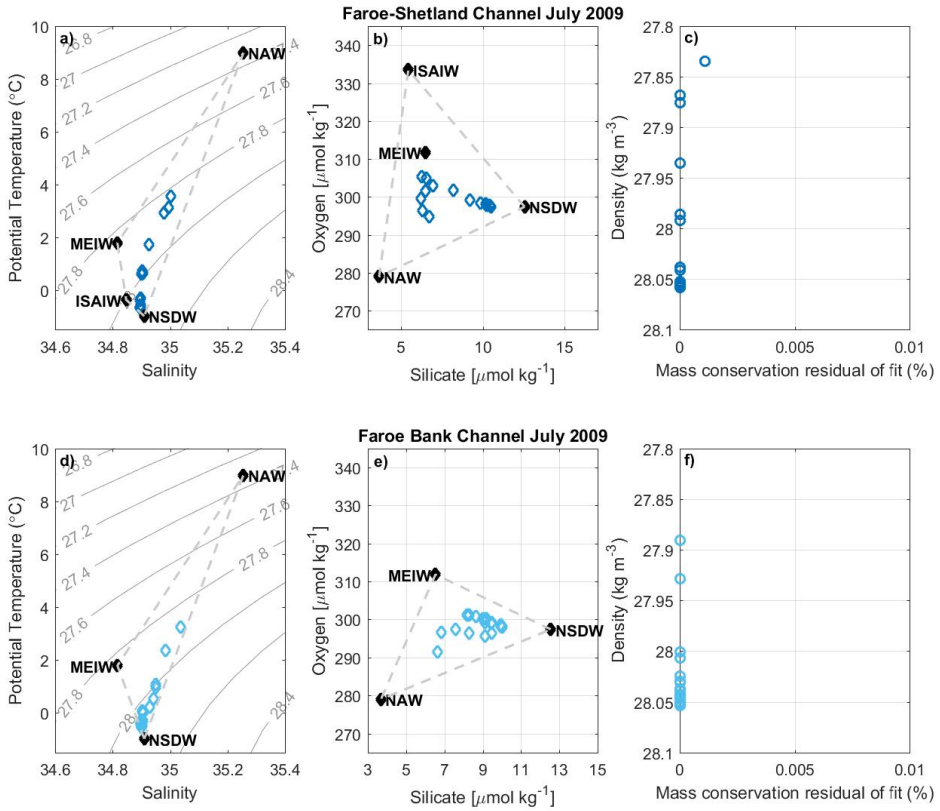

Figure 3.12: The observed data of outflow water ($\sigma_\theta \geq 27.8 \text{kgm}^{-3}$) in the Faroe-Shetland Channel (dark blue diamonds in a-c) and Faroe Bank Channel (light blue diamonds in d-f) in July 2009. The data is plotted in salinity against potential temperature in a) and d) with isopycnals (gray lines) and mixing lines (gray dashed lines), and in silicate against oxygen in b) and e) including mixing lines. The mean values for the source waters MNAW, MEIW, ISAIW, and NSDW (black diamonds) are indicated. The resulting mass conservation residual of fit vs. density of the extended OMP analyses are shown in c) and f).

In April 2015 the hydrochemical nearly all observational data is still encircled by the mixing lines spanned out by MNAW, MEIW, ISAIW, and NSDW (Fig.3.13). One data point falls outside the spanned silicate-oxygen space in the Faroe-Shetland Channel, while one data point is left outside the mixing lines in the TS-diagram in the Faroe Bank Channel. The outflow water should by the looks of the parameter spaces continue to be well described by the source water combination. Compared to the two previous time periods, the mass conservation residuals have increased. The residuals are the largest for the densities($\sigma_\theta \geq 28.05 \text{kgm}^{-3}$) in both channels. Little water appears to be well described by the provided source water solution, except for some data in the density interval $28.01 \leq \sigma_\theta \leq 28.05 \text{kgm}^{-3}$ in the Faroe-Shetland Channel. Most

of the outflow was fully resolved using the same source waters in June 2002 and July 2009. Enlarged residuals indicate that the outflow composition and/or the source water properties have undergone a change in April 2015. Note that April 2015 is a different season compared to June 2002 and July 2009, which may have an effect on the outflow.

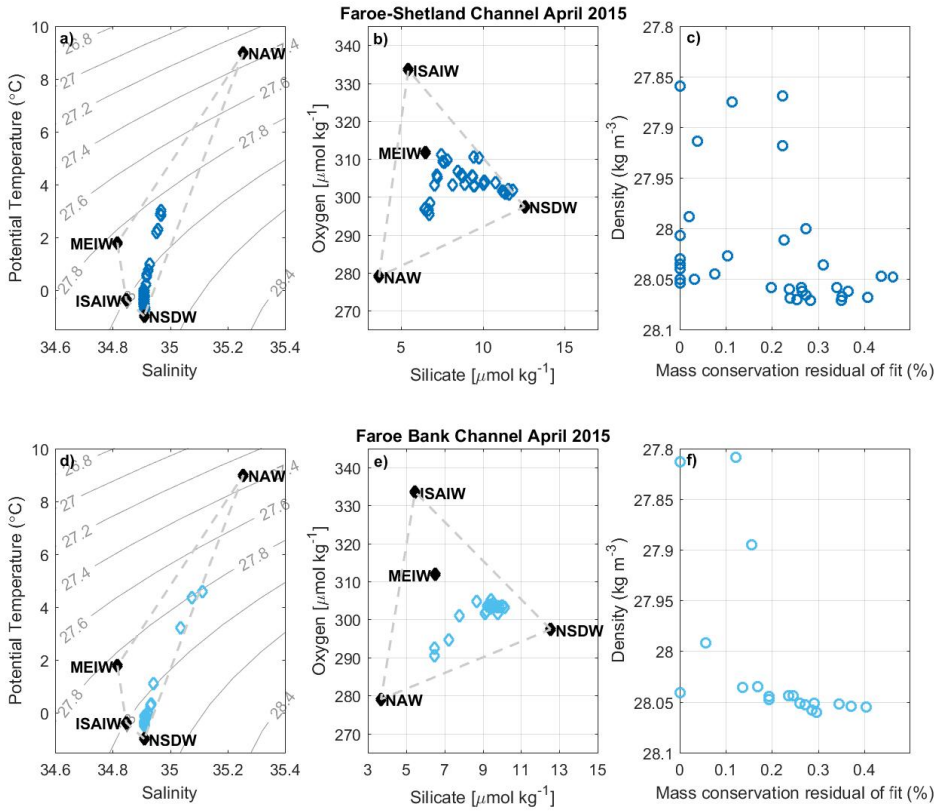

Figure 3.13: The observed data of outflow water ($\sigma_\theta \geq 27.8 \mathrm{kgm}^{-3}$) in the Faroe-Shetland Channel (dark blue diamonds in a-c) and Faroe Bank Channel (light blue diamonds in d-f) in April 2015. The data is plotted in salinity against potential temperature in a) and d) with isopycnals (gray lines) and mixing lines (gray dashed lines), and in silicate against oxygen in b) and e) including mixing lines. The mean values for the source waters MNAW, MEIW, ISAIW, and NSDW (black diamonds) are indicated. The resulting mass conservation residual of fit vs. density of the extended OMP analyses are shown in c) and f).

3.5 Vertical distribution of the source water fractions

Source water fractions are displayed in vertical sections in the Faroe-Shetland Channel for June 2002, July 2009, and April 2015 in Fig.3.14, together with the respective mass conservation residual of fit. The residuals in 2002 and 2009 were low as previously established, while high residuals were found at depth in April 2015. The influence of MNAW was restricted to the upper

part of the outflow in all three sections, with the largest amount found in July 2009. Located at the bottom of the channel was the NSDW, with an additional core at about 700m depth in June 2002. This specific section had the steepest sloping isopycnal, reaching up to a depth of 450m. If the outflow was forced towards the slope, this could allow NSDW to be located at shallower depths. The largest portion of ISAIW was situated between the MNAW and NSDW, with almost no amount detected in the channel in April 2015. Fractions of MEIW were identified mostly in the upper part of the outflow, at same depths as MNAW. However, the amount of MEIW present in the channel in April 2015 increased and the source water was present throughout the outflow. The increase in MEIW could be related to the decrease in ISAIW in April 2015.

Downstream in the Faroe Bank Channel the general picture was the same as in the Faroe-Shetland Channel (Fig.3.15).The mass conservation residuals were low with higher values in April 2015. The presence of MNAW was evident in the upper part of the outflow, although with a deeper penetration than upstream. Amounts of NSDW could here be found throughout the outflow, but with largest contributions at the bottom. This indicated that a mixing of the outflow occurred between the Faroe-Shetland and Faroe Bank Channels. In addition, the depth between the two sites decrease and some recirculation of the denser water is expected. Since NSDW was still present in the Faroe Bank Channel, it indicated that not all of the denser water mass was forced to recirculate upon moving downstream. Some fraction of ISAIW were found throughout the outflow in June 2002, while no presence was resolved in July 2009. In April 2015 the ISAIW appeared in a band at about 650m depth, with small fractions at the bottom of the channel as well. MEIW was situated at all depths in the outflow in all three sections, with an increased contribution in July 2009. This was likely a result of the absence of ISAIW.

3.6 Temporal variation in source water fractions

The contribution of each source water to the total outflow composition is difficult to estimate from their vertical distributions. The total source water fractions of the outflow compositions in both the Faroe-Shetland and Faroe Bank Channels in June 2002, July 2009, and April 2015 are shown in Fig.3.16. The primary component of the outflow were NSDW for both the Faroe-Shetland and Faroe Bank Channels for the three time periods. The source water fractions were similar between the two locations in June 2002, with a slightly enhanced amount of MNAW downstream. In July 2009 there was a decrease in the amount of NSDW in the Faroe-Shetland Channel, which was replaced by ISAIW. It should be noted that the analysis of the Faroe Bank Channel in July 2009 did not resolve any realistic solution when ISAIW was included. However, MEIW intermixes with water from the Iceland Sea when it is transported with the East Icelandic Current. If the fraction of MEIW may represent all water with Icelandic influence, the amount of MEIW found in the Faroe Bank Channel was reduced compared to the summed fractions of MEIW and ISAIW in the Faroe-Shetland Channel in 2009. The source water fractions in April 2015 were similar between the two locations, with a somewhat reduced amount of MEIW and enhanced portion of MNAW in the Faroe Bank Channel. A presence of ISAIW was detected both upstream and downstream in 2015, but the amount could be considered negligible.

Separating the outflow into the same three density layers as earlier gives an indication of the variations within the outflow. In the Faroe-Shetland Channel the fractions of the lightest source waters MNAW and MEIW naturally decreased for increasing densities, while the dense NSDW increased (Fig.3.17). In the lightest part of the outflow the source waters ISAIW and MEIW with Icelandic origin were the largest components. This shifted in the middle layer, where presence of NSDW dominated with further enhanced fractions in the densest layer. In June 2002 and July 2009 the fraction of ISAIW stood out as the second most influential in two deeper

density intervals. This changed in April 2015, which had only small contributions of ISAIW. MEIW seemed to replace ISAIW as the second largest component in the outflow this month. The amount of MEIW still decreased for increasing densities as before, but due to an enlarged presence the deepest interval contained 25% of MEIW compared to 5% in 2002 and 2009. The general distribution of source water fractions in the Faroe Bank Channel was similar to the Faroe-Shetland Channel (Fig.3.18). The influence of MNAW was greatest at low densities and NSDW at high densities. The fractions of ISAIW and MEIW generally decreased throughout the outflow moving downstream, while the amount of MNAW increased. The bulk of ISAIW in July 2009 observed upstream, has here been replaced by MEIW. This is possibly an artefact produced by the analysis, since there is no obvious reason why ISAIW should disappear moving downstream. A homogenization between MEIW and ISAIW as they flow toward the Faroe Bank Channel could have made it difficult for the analysis to distinguish ISAIW.

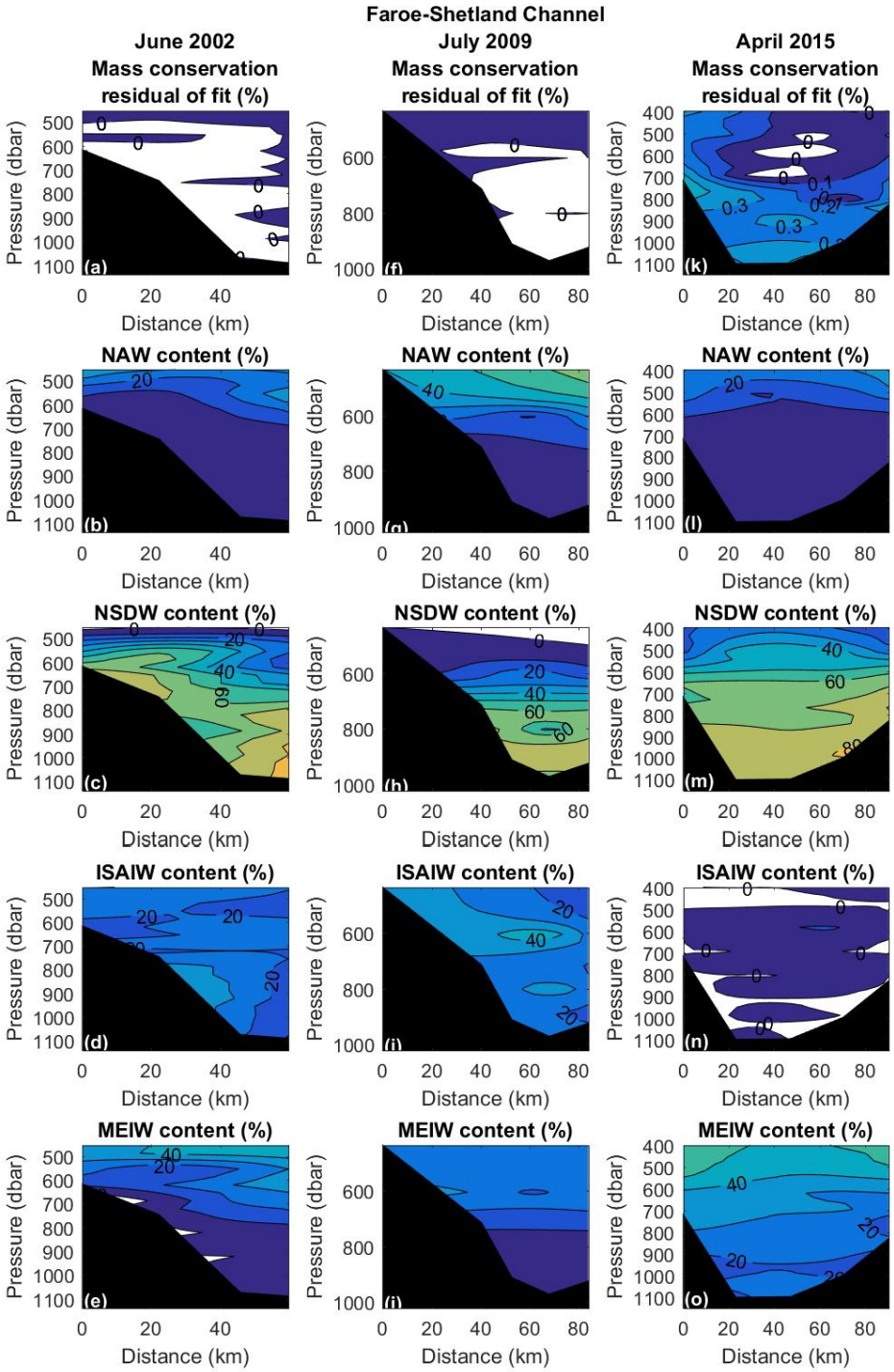

Figure 3.14: Mass conservation residual of fit of the source water composition MNAW, MEIW, NSDW, and ISAIW for outflow water ($\sigma_\theta \geq 27.8 \mathrm{kgm}^{-3}$) in the Faroe-Shetland Channel, together with source water fractions in vertical sections of June 2002 (a-e), July 2009 (f-j), and April 2015 (k-o).

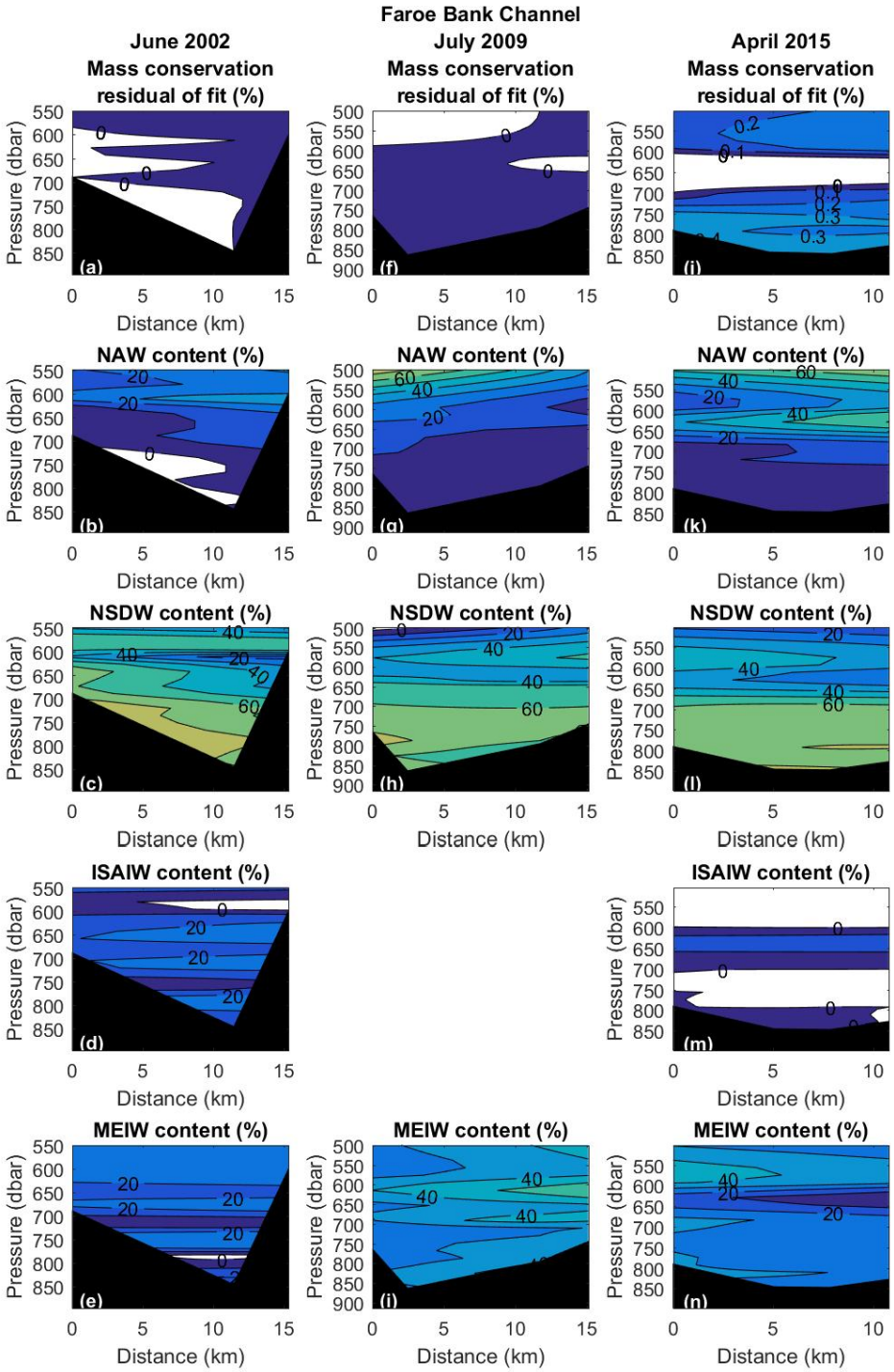

Figure 3.15: Mass conservation residual of fit of the source water composition MNAW, MEIW, NSDW, and ISAIW for outflow water ($\sigma_\theta \geq 27.8 \mathrm{kgm}^{-3}$) in the Faroe Bank Channel, together with source water fractions in vertical sections for June 2002 (a-e), July 2009 (f-i), and April 2015 (j-n).

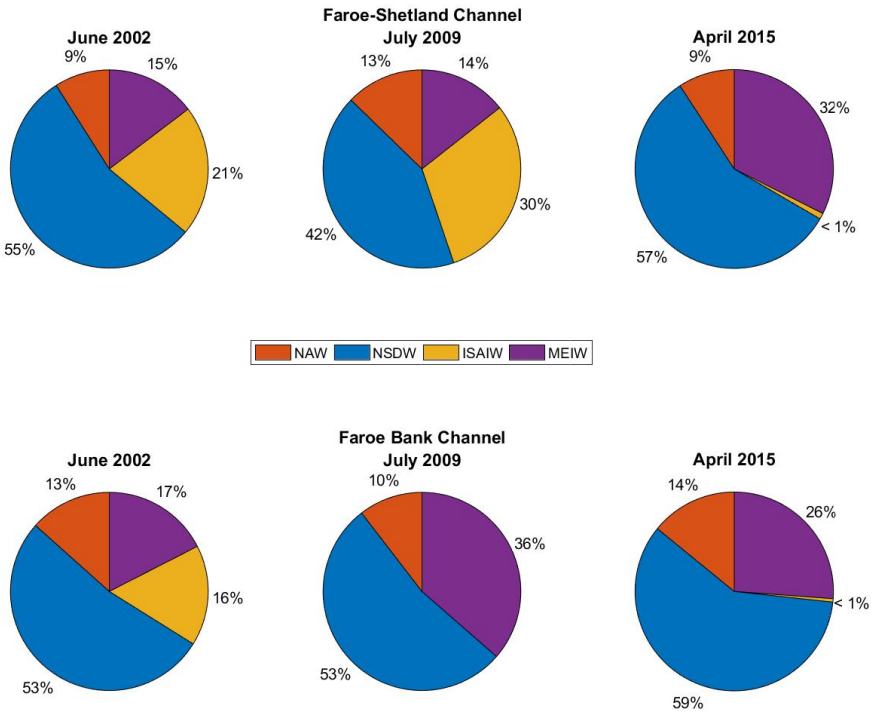

Figure 3.16: Source water fractions of the outflow water ($\sigma_\theta \geq 27.8 \mathrm{kgm}^{-3}$) in the Faroe-Shetland and Faroe Bank Channels in June 2002, July 2009, and April 2015. The percentages of the source waters MNAW (red), MEIW (purple), ISAIW (yellow), and NSDW (blue) rounded off and given.

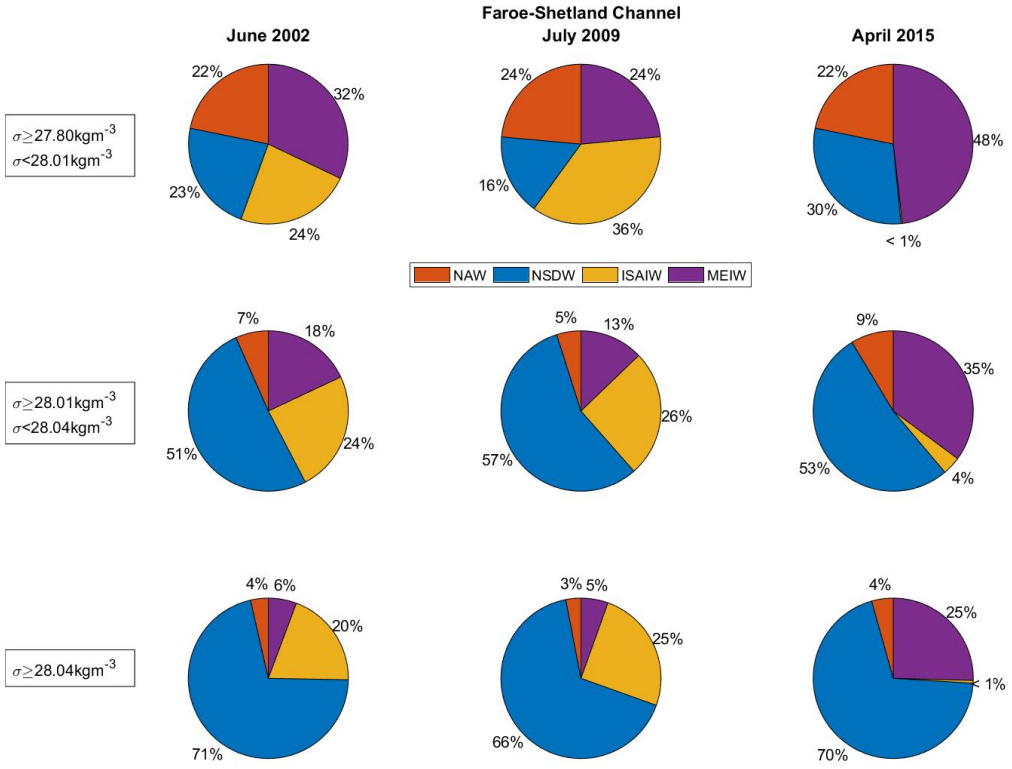

Figure 3.17: Source water fractions of the three outflow density layers separated into the three density layers $27.80 \leq \sigma_\theta < 28.01 \mathrm{kgm}^{-3}$ (top), $28.01 \leq \sigma_\theta < 28.04 \mathrm{kgm}^{-3}$ (middle), and $\sigma_\theta \geq 28.04 \mathrm{kgm}^{-3}$ (bottom) in the Faroe-Shetland Channel in June 2002, July 2009, and April 2015. The percentages of the source waters MNAW (red), MEIW (purple), ISAIW (yellow), and NSDW (blue) are rounded off and given.

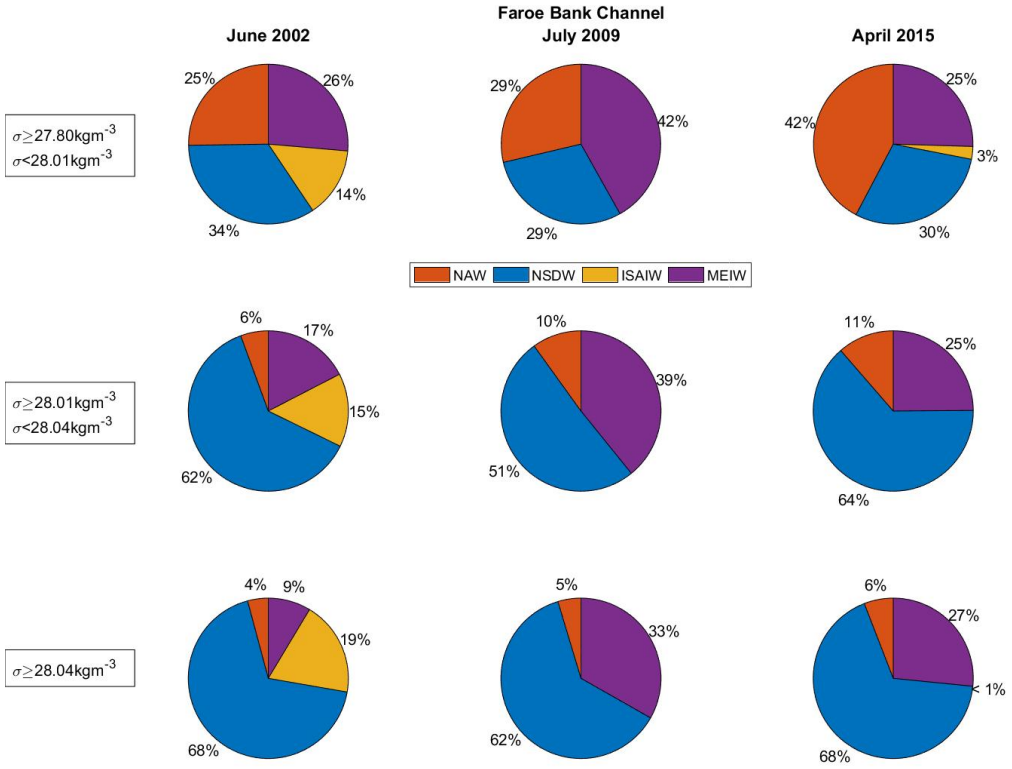

Figure 3.18: Source water fractions of the three outflow density layers separated into the three density layers $27.80 \leq \sigma_\theta < 28.01 \mathrm{kgm}^{-3}$ (top), $28.01 \leq \sigma_\theta < 28.04 \mathrm{kgm}^{-3}$ (middle), and $\sigma_\theta \geq 28.04 \mathrm{kgm}^{-3}$ (bottom) in the Faroe Bank Channel in June 2002, July 2009, and April 2015. The percentages of the source waters MNAW (red), MEIW (purple), ISAIW (yellow), and NSDW (blue) are rounded off and given.

Chapter 4

Discussion

While the general structure is conserved, the water properties change between the Faroe-Shetland and Faroe Bank Channels. Moving downstream, the steep gradients across the outflow interface are compressed with a 300m thick well-mixed layer overhead. This homogeneous layer is observed for all three time periods, indicating work done by stable processes. Mixing, entrainment, and recirculation are processes which may produce such a layer, and have been discussed to take place between the Faroe-Shetland Channel and the Faroe Bank sill [Mauritzen et al., 2005]. Current shear from an opposite flow direction at the surface and bottom of the channels induce mixing in the interior. Mauritzen et al. (2005) theorizes that intense mixing in the channel is due to resonance with tidal induced internal waves. A decreasing water column depth moving downstream from the Faroe-Shetland Channel towards the sill implies recirculation of the deepest water. The importance of the individual processes are disagreed upon. Discontinuities in the properties of MEIW between the Faroe-Shetland and Faroe Bank Channel, lead Turrell et al. (1999) to assume that recirculation takes place in the Faroe-Shetland Channel. On the other hand, Saunders (1990) considered the MEIW to follow the channel and be strongly altered by mixing. Examining the importance of the individual processes is beyond the scope of this thesis, but a result of mixing between the two sites is observed.

The outflow wate ($\sigma_\theta \geq 27.8 \text{kgm}^{-3}$) in the Faroese Channels is well described by NSDW, ISAIW, MEIW, and MNAW, or a combination thereof, for the three months June 2002, July 2009, and April 2015. Previous studies all agreed on NSAIW as one of the contributing water sources. However, NSAIW is influenced by both GSAIW and ISAIW, and of the two it seems more likely to observe ISAIW in the channel system since the East Icelandic Current brings it to the entrance.

Different inflows of Atlantic water in the Faroe-Shetland and Faroe Bank Channels cause dissimilarities between the two locations. The lightest layer of the outflow which is most susceptible to be influenced by the Atlantic surface water, saw a clear increase in both temperature and salinity in the Faroe Bank Channel in April 2015 with only a steady salinity increase in the Faroe-Shetland Channel. The general Atlantic inflow to the Nordic Seas have seen a warming and salinification since the 1990s [Holliday et al., 2008]. Hansen et al. (2015) established that the Atlantic transport increased from 1993 to 2013. An increased transport could explain the increased Atlantic influence found in the Faroe Bank Channel, which is more directly influenced by the Atlantic inflow crossing the Iceland-Faroe Ridge. The change in season between the 2002/2009 and 2015 data, would give lower surface temperatures in spring whereas the lightest part of the outflow experience a 1^circc temperature increase. Source water fractions further indicate an increased contribution of Atlantic water at the site.

An increase in oxygen content in April 2015 is evident in the outflow water in vertical sections of both the Faroe-Shetland and Faroe Bank Channels. Enhanced values are reflected in the temporal evolution of the water properties for the two denser outflow layers, indicating the presence of a source water with densities $\sigma_\theta \geq 27.8 \text{kgm}^{-3}$ with high oxygen content. The source water fractions in 2015 reveal a near absence of ISAIW, which previously has been quite influential. It is replaced by an increased fraction of MEIW, which is defined with a mean temperature of 1.78°C and mean salinity of 34.81. This should have induced a warming and freshening of the denser layers of the outflow, where a slight warming and a salinification is observed. Increased mass conservation residuals further imply contribution from a source water not included in the analysis, even though the criteria for a valid solution is satisfied by low residual values. Possible candidates are NSAIW and GSAIW, which have similar mean temperatures and salinities to the observed values in the denser layers of the outflow. With the source water definitions from 2002, the best fit appears to be GSAIW with its high oxygen content. This would demonstrate a variation in the outflow composition and mean that the supply of water to the channel is not constant, due to interchanging processes taking place in the Nordic Seas.

A high fraction of NSDW at about 700m depth in 2002 could have been elevated to this position by strong flow, indicated by a steep sloping isopycnal. Another possible explanation is the creation of an artefact by the analysis. If the water at this location has characteristics which fall outside the mixing of the selected source waters, the analysis will fill in what is missing with a fraction of source water which might physically make little sense. However, all observed data is encircled by the source waters selected for the analysis. Thus, NSDW has likely been misplaced by forcing in this case, even though it is expected to be confined to the bottom of the channels.

The contribution of ISAIW to the Faroese outflow in 2009 appear to vanish between the Faroe-Shetland and Faroe Bank Channels. Partly recirculation in intermediate waters can be expected [Turrell et al., 1999], as the water column compresses toward the Faroe Bank Channel. With intense mixing between MEIW and ISAIW, these could have been homogenized and made them inseparable to the analysis. Inspecting the parameter space, the observed data in the Faroe Bank Channel is spanned by just including MEIW, NSDW, and MNAW in the composition, without any influence by ISAIW on MEIW. Without any physical explanation to why ISAIW disappear between the two locations, it seems probable that the analysis provide an unrealistic solution to the outflow composition in the Faroe Bank Channel in 2009. MEIW and ISAIW are the two source waters with the highest deviations in definitions, likely influenced by local variability in forcing and season in the Iceland Sea.

The fractions of source waters overall and in the respective density layers of the Faroese outflow appear fairly stable between 2002, 2009, and 2015. No clear temporal variation or trends in source water fractions imply a reliable result. Larger variation would indicate larger uncertainties. NSDW is observed throughout the overflow layers and is the dominating source water in the deeper parts (>50%), considering both temporal and spatial evolution. With a fraction ranging between 42% to 59% in the channels, there are no evident signs of reducing deep water formation in the Nordic Seas which could affect the AMOC. However, the deep water reservoirs would take some time to drain in the event of a shutdown. This would reduce deep water layers and consequently bring the interface below the mouth of the Faroese Channels, inhibiting deep water entering. Then there should be signs ofdeep water decline in the temporal variability of the overflow if the deep water basins were being drained. Turrell et al. (1999) found the deep water in the Faroe-Shetland Channel to compose of 60% NSDW during the time period 1970-1985, while the fraction decreased to 40% during the years 1990 to 1995. With 42-57% contribution of NSDW in the Faroe-Shetland Channel, it seems to be the other way around with an increased deep water supply to the channels. However, these values originate from snapshots of the channel at specific times, while Turrell et al. (1999) extracted their fractions

from long observation periods. A direct comparison may therefore not be justifiable, but the values presented here could give an indication of a re-established fractions of NSDW.

4.1 Uncertainties

The observational data for the period 2002-2015 are sparse, with only three transects taken in each of the Faroese Channels. Due to seasonal variability, interannual studies should ideally be chosen for the same month [Holliday, 2008]. There was no opportunity presented for an optimal interannual comparison as the observations were made during three different months and at changing locations. Thus, any trends in water properties derived from these measurements are with some uncertainty.

Errors in the OMP analysis are related to seasonal and interannual variability, source water definitions, and data measurements. With the potential of many water masses compressed into the water column of the Faroese Channels, the analysis might not have resolved the correct composition. With source regions in the Nordic Seas closely grouped, the source waters interact and could prove difficult to isolate for definitions. Little observational data is provided to define MEIW, resulting in high standard deviations and introducing error to the analysis as it appears to be an important contributor to the outflow composition.

Chapter 5

Conclusion

Changes were observed in water column properties between the Faroe-Shetland and Faroe Bank Channel, influenced by the difference in Atlantic inflows and by mixing processes between the two location. There was a clear seasonal shift between 2002/2009 and 2015 in the surface of channels. Despite temporal and spatial variations, the composition of the deep outflow in the Faroese Channels could be described by NSDW, ISAIW, MEIW, and MNAW in all periods with data; June 2002, July 2009, and April 2015. From available observations, the outflow in the Faroese Channels increased in salinity and increased slightly in temperature in the Faroe Bank Channel. Source water fractions revealed an increased Atlantic influence in the Faroe Bank Channel. A near absence of ISAIW in 2015 in both channels together with increased mass conservation residuals and enhanced oxygen content indicate the presence of another source water. With a variable outflow composition, the water from the Nordic Seas could play a crucial part in the changes of AMOC. However, source water fractions provide no evidence of a declining contribution of deep waters to the Faroese outflow, suggesting a stable supply of dense water through the Faroese Channels to the North Atlantic Ocean.

Chapter 6

References

Aagaard, K. and Carmack, E. (1989). The role of sea ice and other fresh water in the Arctic circulation. Journal of Geophysical Research, 94(C10), p.14485.

Aagaard, K., Swift, J. and Carmack, E. (1985). Thermohaline circulation in the Arctic Mediterranean Seas. Journal of Geophysical Research, 90(C3), p.4833.

Blindheim, J. (1990). Arctic intermediate water in the Norwegian sea. Deep Sea Research Part A. Oceanographic Research Papers, 37(9), pp.1475-1489.

Blindheim, J. and Rey, F. (2004). Water-mass formation and distribution in the Nordic Seas during the 1990s. ICES Journal of Marine Science, 61(5), pp.846-863.

Borens, K. and Lundberg, P. (1988). On the deep-water flow through the Faroe Bank Channel. Journal of Geophysical Research, 93(C2), p.1281.

Buch, E., Malmberg, S. and Kristmannsson, S. (1996). Arctic Ocean deep water masses in the western Iceland Sea. Journal of Geophysical Research: Oceans, 101(C5), pp. 11965-11973.

Caesar, L., Rahmstorf, S., Robinson, A., Feulner, G. and Saba, V. (2018). Observed fingerprint of a weakening Atlantic Ocean overturning circulation. Nature, 556(7700), pp.191-196.

Curry, R. and Mauritzen, C. (2005). Dilution of the Northern North Atlantic Ocean in Recent Decades. Science, 308(5729), pp.1772-1774.

Dickson, R., and Brown, J. (1994). The production of North Atlantic Deep Water: Sources, rates, and pathways. Journal of Geophysical Research, 99(C6), p.12319.

Eldevik, T., Nilsen, J., Iovino, D., Anders Olsson, K., Sandø, A. and Drange, H. (2009). Observed sources and variability of Nordic seas overflow. Nature Geoscience, 2(6), pp.406-410.

Fogelqvist, E., Blindheim, J., Tanhua, T., Østerhus, S., Buch, E. and Rey, F. (2003). GreenlandScotland overflow studied by hydro-chemical multivariate analysis. Deep Sea Research Part I: Oceanographic Research Papers, 50(1), pp.73-102.

Hansen, B., Larsen, K., Htn, H., Kristiansen, R., Mortensen, E. and sterhus, S. (2015). Transport of volume, heat, and salt towards the Arctic in the Faroe Current 19932013. Ocean Science, 11(5), pp.743-757.

Hansen, B., Turrell, W. and Østerhus, S. (2001). Decreasing overflow from the Nordic seas into the Atlantic Ocean through the Faroe Bank channel since 1950. Nature, 411(6840), pp.927-930.

Hansen, B., and Østerhus, S. (2000). North Atlantic-Nordic Seas exchanges. Progress in Oceanography, 45, pp.109-208.

Helland-Hansen, B. (1916). Nogen hydrografiske metoder. (Some hydrographical methods).

Holliday, N., Hughes, S., Bacon, S., Beszczynska-Mller, A., Hansen, B., Lavn, A., Loeng, H., Mork, K., Østerhus, S., Sherwin, T. and Walczowski, W. (2008). Reversal of the 1960s to 1990s freshening trend in the northeast North Atlantic and Nordic Seas. Geophysical Research Letters, 35(3).

Hurdle, B. (1986). The Nordic seas. New York: Springer-Verlag.

Jochumsen, K., Moritz, M., Nunes, N., Quadfasel, D., Larsen, K., Hansen, B., Valdimarsson, H. and Jonsson, S. (2017). Revised transport estimates of the Denmark Strait overflow. Journal of Geophysical Research: Oceans, 122(4), pp.3434-3450.

Jeansson, E., Olsen, A. and Jutterstrm, S. (2017). Arctic Intermediate Water in the Nordic Seas, 19912009. Deep Sea Research Part I: Oceanographic Research Papers, 128, pp.82-97.

Karstensen, J. and Tomczak, M. (1998). Age determination of mixed water masses using CFC and oxygen data. Journal of Geophysical Research: Oceans, 103(C9), pp.18599-18609.

Karstensen, J. (2005). Water mass transformation in the Greenland Sea during the 1990s. Journal of Geophysical Research, 110(C7).

Kuhlbrodt, T., Griesel, A., Montoya, M., Levermann, A., Hofmann, M. and Rahmstorf, S. (2007). On the driving processes of the Atlantic meridional overturning circulation. Reviews of Geophysics, 45(2).

Leffanue, H. and Tomczak, M. (2004). Using OMP analysis to observe temporal variability in water mass distribution. Journal of Marine Systems, 48(1-4), pp.3-14.

Macrander, A. (2005). Interannual changes in the overflow from the Nordic Seas into the Atlantic Ocean through Denmark Strait. Geophysical Research Letters, 32(6).

Macrander, A., Valdimarsson, H. and Jnsson, S. (2014). Improved transport estimate of the East Icelandic Current 2002-2012. Journal of Geophysical Research: Oceans, 119(6), pp.3407-3424.

Marshall, J. and Schott, F. (1999). Open-ocean convection: Observations, theory, and models. Reviews of Geophysics, 37(1), pp.1-64.

Mackas, D., Denman, K. and Bennett, A. (1987). Least squares multiple tracer analysis of water mass composition. Journal of Geophysical Research, 92(C3), p.2907.

Mauritzen, C., Price, J., Sanford, T., and Torres, D. (2005). Circulation and mixing in the Faroese Channels. Deep-Sea Research I, 52, pp.883-913.

Mauritzen, C. (1996). Production of dense overflow waters feeding the North Atlantic across the Greenland-Scotland Ridge. Part 1: Evidence for a revised circulation scheme. Deep-Sea Research I, 43, pp.769-806.

Olsen, A., Key, R.M., van Heuven, S., Lauvset, S.K., Velo, A., Lin, X., Schirnick, C., Kozyr, A., Tanhua, T., Hoppema, M., Jutterstrm, S., Steinfeldt, R., Jeansson, E., Ishii, M., Prez, F.F., and Suzuki, T. (2016). The Global Ocean Data Analysis Project version 2 (GLODAPv2) an internally consistent data product for the world ocean. Earth Syst. Sci. Data, 8, pp.297-323.

Rudels, B., Bjrk, G., Nilsson, J., Winsor, P., Lake, I. and Nohr, C. (2005). The interaction between waters from the Arctic Ocean and the Nordic Seas north of Fram Strait and along the East Greenland Current: results from the Arctic Ocean-02 Oden expedition. Journal of Marine Systems, 55(1-2), pp.1-30.

Rudels, B., Fahrbach, E., Meincke, J., Budus, G., Eriksson, P., 2002. The East Greenland Current and its contribution to the Denmark Strait overflow. ICES J. Mar. Sci. 59 (6), 11331154. http://dx.doi.org/10.1006/jmsc.2002.1284.

Sarmiento, J. (2013). Ocean Biogeochemical Dynamics. Princeton: Princeton University Press.

Stefannson, U. (1962). North Icelandic waters. Reykjavik: Atvinnudeild Haskolans, Fiskideild.

Stefnsson, U. (1968). Dissolved nutrients, oxygen and water masses in the Northern Irminger Sea. Deep Sea Research and Oceanographic Abstracts, 15(5), pp.541-575.

Saunders, P. (1990). Cold Outflow from the Faroe Bank Channel. Journal of Physical Oceanography, 20(1), pp.29-43.

Swift, J.H., Aagaard, K., 1981. Seasonal transitions and water mass formation in the Iceland and Greenland seas. Deep-Sea Res. 28A (10), 11071129. http://dx.doi.org/ 10.1016/0198-0149(81)90050-9.

Swift, J. and Koltermann, K. (1988). The origin of Norwegian Sea Deep Water. Journal of Geophysical Research, 93(C4), p.3563.

Tanhua, T., Olsson, K. and Jeansson, E. (2005). Formation of Denmark Strait overflow water and its hydro-chemical composition. Journal of Marine Systems, 57(3-4), pp.264-288.

Tomczak, M. (1981). A multi-parameter extension of temperature/salinity diagram techniques

for the analysis of non-isopycnal mixing. Progress in Oceanography, 10(3), pp.147-171.

Tomczak, M. (1999). Some historical, theoretical and applied aspects of quantitative water mass analysis. Journal of Marine Research, 57(2), pp.275-303.

Tomczak, M., and Large, D.G.B. (1989). Optimum Multiparameter Analysis of Mixing in the Thermocline of the Eastern Indian Ocean. Journal of Geophysical Research, 94, pp.16141-16149.

Turrell, W., Slesser, G., Adams, R., Payne, R., and Gillibrand, P. (1999). Decadal variability in the composition of Faroe Shetland Channel bottom water. Deep Sea Research Part I: Oceanographic Research Papers, 46(1), pp.1-25.

Walker, S., Weiss, R. and Salameh, P. (2000). Reconstructed histories of the annual mean atmospheric mole fractions for the halocarbons CFC-11 CFC-12, CFC-113, and carbon tetrachloride. Journal of Geophysical Research: Oceans, 105(C6), pp.14285-14296.

Wilkenskjeld, S., and Quadfasel, D. (2005), Response of the Greenland-Scotland overflow to changing deep water supply from the Arctic Mediterranean, Geophysical research letters, 32, L21607, doi:10.1029/2005GL024140.

Wunsch, C. (2002). OCEANOGRAPHY: What Is the Thermohaline Circulation?. Science, 298(5596), pp.1179-1181.

Østerhus, S., Turrell, W.R., Hansen, B., Lundberg, P., and Buch, E. (2001). Observed transport estimates between the North Atlantic and the Arctic Mediterranean in the Iceland-Scotland region. Polar research, 20(1), pp.169-175.

Redfield, A.C., Ketchum, B.H., Richards, F.A., (1963). The influence of organisms on the composition of sea-water. In: Hill, M.N. (Ed.), The Sea: Ideas and Observations on Progress in the Study of the Seas, 2, Wiley, London, pp. 26 77.

Våge, K., Moore, G., Jnsson, S. and Valdimarsson, H. (2015). Water mass transformation in the Iceland Sea. Deep Sea Research Part I: Oceanographic Research Papers, 101, pp.98-109.